Centre for Geo-Information

Thesis Report GIRS-2005-04

Imaging Spectroscopy for Ecological Monitoring at the Test Site the Millingerwaard: Species Mapping using Spectral Libraries and Soil-Vegetation-Atmosphere-Transfer Models

Elisa Liras Laita

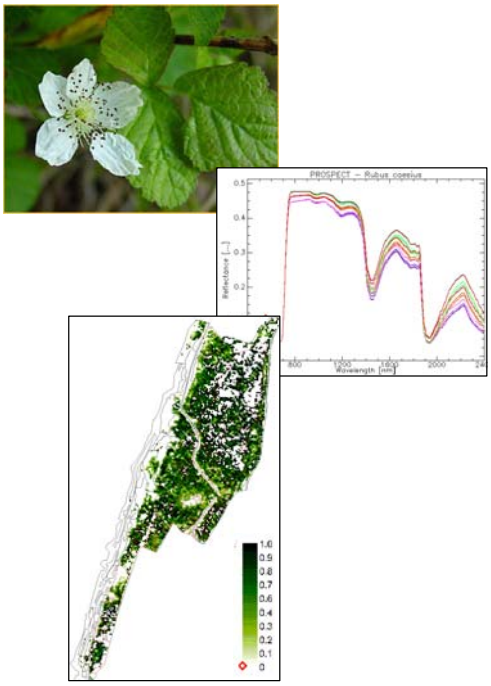

May 2005

WAGENINGEN UNIVERSITY
WAGENINGEN UR

Imaging Spectroscopy for Ecological Monitoring in the Test Site the Millingerwaard: Species Mapping using Spectral libraries and Soil-Vegetation-Atmosphere-Transfer Models

Elisa Liras Laita

Registration number 81 01 22 523 080

Supervisors:

Prof. Dr. sc. nat. Michael E. Schaepman
Dr. ir. Lammert Kooistra

A thesis submitted in partial fulfillment of the degree of Master of Science at Wageningen University and Research Centre, The Netherlands.

May 2005
Wageningen, The Netherlands

Thesis code number: GRS-80337
Wageningen University and Research Centre
Laboratory of Geo-Information Science and Remote Sensing
Thesis Report: GIRS-2005-04

SUMMARY

Considering actual urban and industrial development, in addition to plant and animal production, ecosystems within developed countries are suffering a decrease in biodiversity. Thus, one of the main interests of the governments is to preserve the natural ecosystems.
Certain vegetation communities have a high ecological response to changes in the environment, as temperature or precipitation. Then, they can be used as indicators when possible temporal changes are occurring the environment.

Ecological models have proved to be a potential tool to monitor the vegetation, in order to preserve natural species and predict future ecosystems development. In addition, remote sensing technologies offer the possibility to retrieve valuable inputs data for these models, considering not only abiotic but also biotic parameters.

The presented study has been carried out over a test site named the Millingerwaard, an area closed to Nijmegen, The Netherlands.

Hyperspectral data were collected in the field for the main species in the Millingerwaard, as well as airborne images from the HyMap sensor.
The coupled model PROSAIL has been used to retrieve biochemical and biophysical parameters of the species of interest, as well as to simulate reflectance spectra at the leaf and canopy levels.
Using these results to analyze the hyperspectral images, linear spectral unmixing has been applied to map species abundances over the study area.
Additionally, spectral libraries for the dominant species, from ecological and spatial point of view, have been built up for its radiometric characterization.

As a result, abundance maps for 6 vegetation species have been produced. In general, obtained abundances appear as a good indicator for the spatial coverage of the species. Furthermore, the accuracy of reliability of the results increases when grouping the species according to their structural properties.

In this way, this study sets up the first steps to retrieve spatial information over the test site, for single species, using ecological models and imaging spectroscopy techniques.

TABLE OF CONTENTS

APPENDICES

LIST OF FIGURES

APPENDICES

LIST OF TABLES

APPENDICES

ABBREVIATIONS

- ALA: Average Leaf Angle [degrees]
- C_{ab}: chlorophyll a and b content [$\mu g/cm^2$]
- C_b: brown pigments content [$\mu g/cm^2$]
- C_m: dry mass content [g/cm^2]
- C_w: leaf water content [g/cm^2]
- EWT: Equivalent Water Thickness [cm]
- LAI: Leaf Area Index [m^2/m^2]
- N: foliar structure [number of elementary layers]
- Rad: radians
- RMS: Root Mean Square
- SAIL: Scattering by Arbitrarily Inclined Leaves
- ULSU: Unconstrained Linear Spectral Unmixing
- FCLSU: Fully Constrained Linear Spectral Unmixing
- s_l: hot spot parameter
- ρ: reflectance
- Lρ: leaf reflectance
- Cρ: canopy reflectance

1- INTRODUCTION

1.1- Background

The Millingerwaard (The Netherlands) is a floodplain along the Waal river. As part of the Gelderse Poort natural reserve, one of its main characteristics is the high biodiversity. Thus, it is important to monitor and predict future ecosystem evolution, as part of an integrated plan to protect nature over developed countries.

In a parallel way, due to the technological improvement during the last decades, remote sensing science has developed and new applications have been set up. So that, hyperspectral data has been used for vegetation detection and characterisation.

Biochemical and biophysical parameters for the vegetation can be retrieved from hyperspectral imagery, and later on, implemented on ecological model. Then, vegetation biodiversity can be regularly monitored without and extensive field work campaign. Consequently, future ecosystem development can be predicted.

1.2- Objectives

Radiative transfer models simulate the radiation transfer processes within the system canopy- atmosphere in an accurate way for certain parameters. Taking into account the biochemical and biophysical properties of the vegetation, they model its reflectance properties. Thus, considering biochemical and biophysical variables, accurate vegetation monitoring and species distribution can be assessed.

Remote sensing and hyperspectral imagery offers a potential tool to retrieve reliable estimations of the needed parameter (Curran, 1999), in order to input them in the mentioned ecological models.
Then, combining ecological models with remote sensing procedures, allows ecological mapping.

The main objective of the present study is to retrieve spectral unique information for the present vegetation species, in order to asses an accurate land classification regarding biophysical and biochemical determining parameters.

1.3- Research questions

In order to fulfil the objectives of the study, spectral libraries for the more extent species in the Millingerwaard will be built.
However, not only the present species but its location and quantity are important to characterise ecosystems biodiversity. Consequently, abundance maps for each species will be produced.

To assess future monitoring of the study area, biophysical and biochemical parameters have to be retrieved, and its influence on the reflectance spectra would be investigated.
So, as a conclusion of the present study, vegetation species of the study area will be spectrally characterised, as well as its biochemical and biophysical properties will be derived from this information.
Abundance maps per species will be presented in the final results, and more important possible vegetation communities in the area will be spectrally investigated for future research.

1.4- Thesis Structure

This report is divided in eight chapters. First chapter presents an introduction to the study. It establishes the problem definition and describes the main objectives of the present study.
Second chapter describes the basic principles of imaging spectroscopy for vegetation mapping, radiative transfer models and linear mixture analysis, in order to understand the applied methodology, and the current status of the topic within the scientific community.
Third chapter goes through the available data and techniques to fulfil the objectives. The methodology of the study is also included in this chapter, and presented as a chain of steps.
Fourth chapter shows the obtained results after data processing, and gives a brief explanation on them. In chapter five, final conclusions are made, especially about the importance and quality of the obtained results.
Chapter six consists on an outlook, divided in two sections. In the first one, possible improvements to the present methodology are proposed. On the second section, a list of ideas to continue on the research from the obtained results is given.
Chapters seven and eight include the acknowledgements and references of the study.
Finally, at the end of the report, the appendices on which the text makes references can be found.

2- IMAGING SPECTROSCOPY, RADIATIVE TRANSFER MODELS AND LINEAR SPECTRAL UNMIXING

2.1- Introduction

This chapter provides an overview on the basic principles of the scientific methodology, in order to understand and apply the present study.
First, the basic applications of imaging spectroscopy for mapping vegetation are described, as well as the current status of the scientific research is settle down. Secondly, a brief explanation on radiative transfer models used on this study is shown, to justify later assumptions and decisions.
Finally, an explanation on Linear Spectral Unmixing procedure is given.

2.2- Imaging Spectroscopy

2.2.1- Vegetation mapping

Remote sensing images have been widely used for vegetation detection and classification (Thomas *et al.*, 2002; Calvao and Palmeirim, 2004, Ingram, 2004). One of the main interests of actual scientific community is to map vegetation. Further more, hyperspectral imagery has the advantage of been a potential tool for vegetation parameter retrieval.

Biochemical and biophysical parameters have been investigated from high spectral resolution images (Clevers, 1988, Jago *et al.*, 1999; Coops *et al.*, 2003; Schaepman *et al.*, 2004). On this frame, species detection can be performed to map invasive species or monitor vegetation series along the time (Underwood *et al.*, 2003). On the other hand, the retrieval of biochemical and biophysical parameters can be used in fire assessment studies (Gillon, 1997; Jacquemoud and Ustin, 2004) and to detect different stress states of the vegetation (Curran *et al.*, 2001).
As a summary, water content, dry biomass and chlorophyll content are usually the most interesting parameters (Sims, 2002).

Additionally, hyperspectral imagery, by means of parameter retrieval, provides valuable input data to apply and validate ecological modelling, to investigate and predict biodiversity state and evolution within vegetal ecosystems (Curran *et al.*, 2001; Rahman, 2002).

2.2.2- Spectral libraries

Spectral libraries are collections of reflectance spectra measured from materials of known composition, usually in the field or laboratory. Habitually, when performing a field work campaign, radiometric measurements on the study area are taken. These collected data are then put under different processes to asses its quality. Once the quality control has been finished, the most common way of storing this spectral information is by means of spectral libraries.

n the present study, ENVI 4.0 software is used to build up several spectral libraries, considering different level reflectance spectra (foliage, canopy), location, species and vegetation communities.

2.3- Radiative transfer models

Radiative transfer models simulates the radiation transfer processes within the system canopy- atmosphere in an accurate way for certain parameters (Verhoef and Bach, 2003).

The PROSPECT model (Jacquemoud and Baret, 1990) simulates the reflectance of a single leave from the input of biochemical parameters: foliar structure (N), chlorophyll a and b content, in $\mu g/cm^2$, (C_{ab}), leaf water content, in g/cm^2 (C_w), brown pigments content, in $\mu g/cm^2$ (C_b) and dry mass content, in g/cm^2 (C_m).
This model is available in several versions, since it has suffered progressive improvements since the 90's, when it was first designed.

The version that will be used in this study takes into account the estimation of chlorophyll (C_{ab}), water content (C_w), dry biomass (C_m), structural characterisation of the leaf (N) and brown pigments content (C_b). All the mentioned parameters can be estimated from ground truth data (leaf reflectance spectrum) and existing literature (Sellers *et al*., 1996), as well as from model inversion.
The obtained "artificial leaf reflectance spectra" will then be used as an input for the Scattering by Arbitrarily Inclined Leaves (SAIL) model (Verhoef, W., 1984), and be validated from the truth data collected during the fieldwork (high accuracy data collected at the canopy level with the Field Spectrometer device).

The SAIL model was first set up in the 80's, and has also been up-dated and optimised during the last decades. The SAIL model uses as an input the leaf reflectance spectra (derived from the PROSPECT model), the soil background spectra (derived from ground data), and certain biophysical parameters used to describe the vegetation (leaf area index *LAI*, the mean leaf inclination angle *ALA*, hot spot parameter s_l, the view zenith angle, the sun zenith angle (rad), the relative azimuth angle, view - sun (rad) and the diffuse fraction).
With these data, the canopy reflectance spectrum is modelled. The output can then be referred as "artificial canopy reflectance", and it represents the canopy characteristics for single vegetation species.

2.3.1- PROSPECT model

The PROSPECT model (Jacquemoud et al., 1996) considers a function that includes chlorophyll a + b concentration (C_{ab}), the leaf water content (C_w), the dry matter content (C_m) and the internal structure parameter (N) as parameters. With the exception of the N parameter, the rest can be physically measured on the leaf.

The way each parameter affects the spectral features of the leaf is at follows: C_w affects the wavelength range from 900 to 2500 nm, N and Cm the entire wavelength range

between 700 and 2500 nm, C_{ab} only the wavelength range between 500 and 700 nm. Thus, the SWIR domain (1500 – 1700 nm) is affected by C_w, N and C_m, and the NIR domain (700 – 900 nm) is only sensitive to N and C_m (Curran, 1989; Fourty *et al.*, 1996).

Some assumptions are done regarding the parameter distribution. Thus, basing our study on previous obtained results (Fourty and Baret, 1998; Grossman *et al*., 1996) C_w can be assumed as logarithmic and N and Cm as linear. In addition, no interactions between parameters are assumed.
In general, the PROSPECT model has proved to yield high accuracy for estimation of water and chlorophyll, medium for carbon based compounds on fresh leaves. Proteins are still on investigation (Fourty and Baret, 1998).

According to previous studies (Jacquemoud *et al*., 1996; Fourty *et al.*, 1996), the leaf optical properties of fresh leave seem to be insensitive to protein. Additionally, cellulose and lignin (or other carbon combinations) is poorly estimated.

2.3.2- SAIL Model

The SAIL radiative transfer model (Verhoef, 1984, 1985) is widespread in the remote sensing community for the estimation of vegetation biophysical variables. It calculates the canopy reflectance, from the leaf reflectance spectra and a limited number of variables describing the plant architecture: The leaf area index *LAI*, the mean leaf inclination angle *ALA*, assuming an ellipsoidal distribution of foliage elements (Campbell, 1990), the hot spot parameter s_l, the view zenith angle, the sun zenith angle (rad), the relative azimuth angle, view - sun (rad) and the diffuse fraction.

2.3.2.1- Parameters description

- *Leaf Area Index:*

Leaf Area Index (LAI) is defined as the one sided green leaf area per unit ground area in broadleaf canopies, or as the projected needle leaf area per unit ground area in needle canopies.

- *Average Leaf Angle:*

The Average Leaf Angle (ALA) is the angle defined between the normal and the vertical for a given leaf. It is mainly a function of the vegetation type, although development stage and sometimes even the solar time have an influence on its value.

- *Hot Spot Parameter:*

Canopy height and leaf size determines the probability of a photon to penetrate a distance z in the canopy. This probability is higher in the illumination direction, which is translated in a higher reflectance in such direction. This phenomenon is known as "hot spot", and it is more important for the red wavelengths than for the NIR (Myneni *et al*., 1995).

- *View Zenith Angle / Sun Zenith Angle (rad) / Relative Azimuth Angle, sun - view (rad):*

View zenith angle is the observation position with relation to the zenith position. Assuming a vertical position of the ASD fibre optic detector, the value is then zero.
Sun zenith angle is the angle that covers the distance (in degrees or radians), between the zenith position and the solar position at the measurement time (*Figure 1*). So that, it can be expressed as:

Sun zenith angle (degrees) = 90° - elevation angle (degrees)

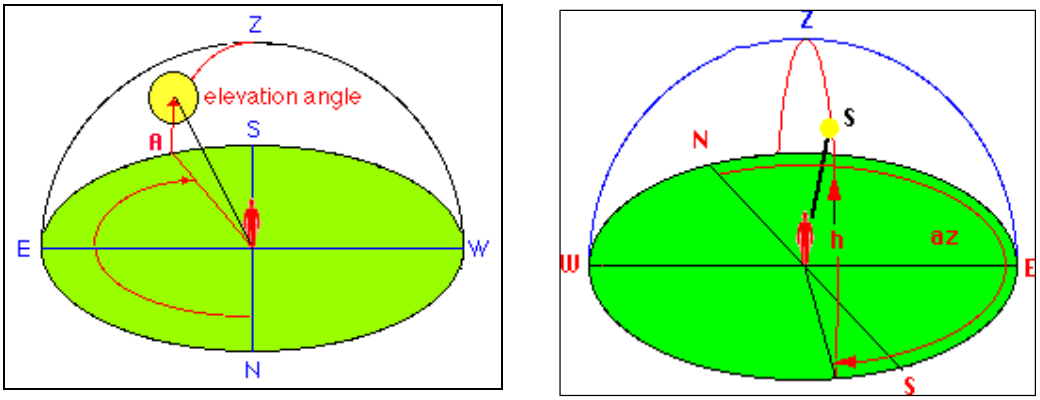

Figure 1: Solar angles

The observer is located at the centre of his "celestial sphere" with zenith Z above his head and the horizon N-E-S-W. The Sun, Moon or any other celestial body can be identified by the two coordinates altitude (elevation) h and azimuth az (horizontal coordinates). Altitude is the angular distance above the horizon (0 < h < 90°), and azimuth the angular distance, measured along the horizon, eastwards from the north point N in nautics (0 < alpha <360°), or westwards from the south point S (in astronomy).

- *Diffuse fraction:*

When a large fraction of the incident light at the top of the atmosphere is transmitted to the ground surface, there is little cloud (and aerosols) and hence, little diffuse light. In contrast, when only a small fraction is transmitted through the atmosphere, a large fraction of the incident light will be diffuse.
For the SAIL model, diffuse fraction has been assumed to be zero. This assumption is made due to the insignificance distance from the virtual spectrometer detector (≈ 50 cm) to the top of the canopy surface in relation with the atmosphere.

2.3.3- PROSPECT - SAIL coupled model

SAIL radiative transfer model is coupled with the PROSPECT model to account for the leaf optical properties. The version used in the present study requires the leaf structure parameter N, the chlorophyll a and b content C_{ab} (µg · cm^{-2}), the equivalent water thickness C_w (cm), the dry matter content C_m (g · cm^{-2}), and the brown pigment

concentration C_b (Jacquemoud and Baret, 1990; Baret and Fourty, 1997), to simulate the leaf reflectance and transmittance spectra in the optical domain.

Considering this coupled model, spectral variations of the contribution of the used variables have been quantified for the reflectance spectrum in the optical domain (Fourty and Baret, 1996): in the visible, the chlorophyll content drives about 50% of the reflectance variations, with a weaker contribution near 550 nm; in the near infrared, the most important variables are the leaf angle parameter and the leaf area index; the middle infrared confirms the strong influence of light absorption by the leaf water content around 1450 and 1940 nm.
The coupled model PROSPECT – SAIL is applied for the estimation of leaf equivalent water thickness, dry matter and leaf structure.

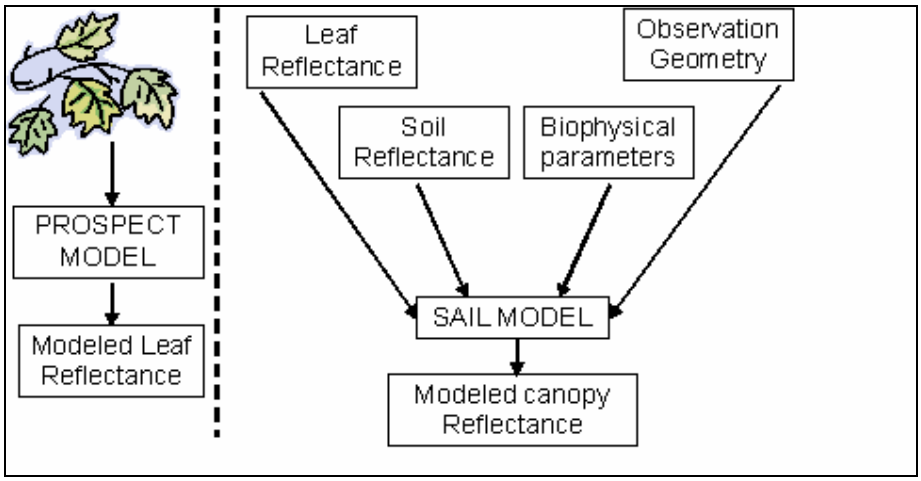

Figure 2: PROSPECT – SAIL coupled model diagram

2.4- Linear Spectral Unmixing

Linear Spectral Unmixing (Adams *et al*., 1986; Boardman, 1989) exploits the theory that the reflectance spectrum of any pixel is the result of linear combinations of the spectra of all endmembers inside that pixel. A linear combination in this context can be thought of as a weighted average, where each endmember weight is directly proportional to the area pixel containing that endmember. If the spectra of all endmembers in the scene are known, then their abundance within each pixel can be calculated from each pixel's spectrum.

Unmixing simply solves a set of *n* linear equations per pixel, where *n* is the number of bands in the image. The unknown variables in these equations are the fractions of each endmember in the pixel.
The result of Linear Spectral Unmixing includes one abundance image for each endmember. The pixel values in these images indicate the percentage of the pixel made up of that endmember.
An error image is also usually calculated to help evaluate the success of the unmixing analysis.

3- MATERIALS AND METHODS

3.1- Introduction

This chapter describes the scientific methodology followed to retrieve the final results. First, an introduction to the study area is given. Then, a description of the available data and the steps to fulfil the modelling approach are described. Finally, the Linear Spectral Unmixing techniques are summarised and justified.
The conceptual model of the applied methodology is shown in *Figures 3 and 4*.

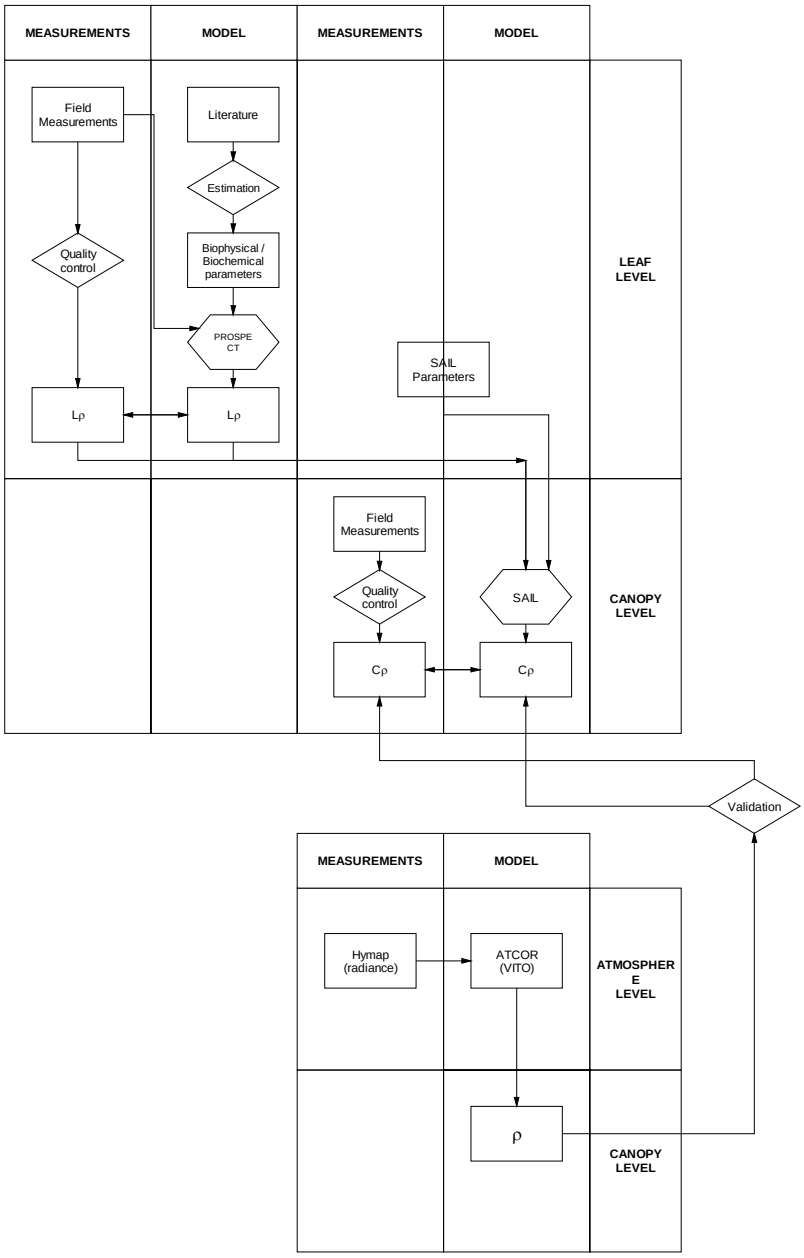

Figure 3: Conceptual model for the modelling steps

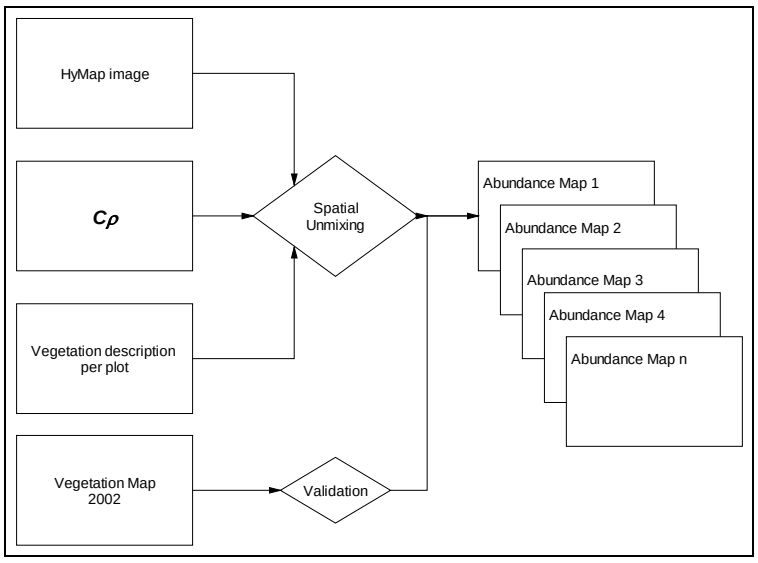

Figure 4: Conceptual model of the mixing / unmixing procedures

3.2- Study area

The study area (*Figure 5*) is located 10 km east of the city of Nijmegen, The Netherlands. The Millingerwaard covers an area of about 700 hectares, 300 of them occupied by pasture areas (*Figure 6*).
It is a floodplain of the Waal river, belonging to the Gelderse Poort natural reserve. Historically, it has been used as a grassland and arable land.

In 1986 the "Plan Ooievaar" was published. In this plan a scenario was proposed for nature development in former flood-plains of the rivers Maas, Rhine and Waal. Purpose is the development of more natural ecosystems by restoring natural processes. In 1989 part of the Millingerwaard was purchased in order to re-initiate more natural processes and to develop "nature". In 1990 all fences were removed and cattle (Galloways in 1992) and horses (Koniks in 1991) were introduced to the area. Since 1994 the vegetation development has been monitored by means of permanent plots and repeated vegetation mapping.
It presents a high biodiversity, considering vegetation species. Shrubs, forest and several types of grasslands species can be found in the area.

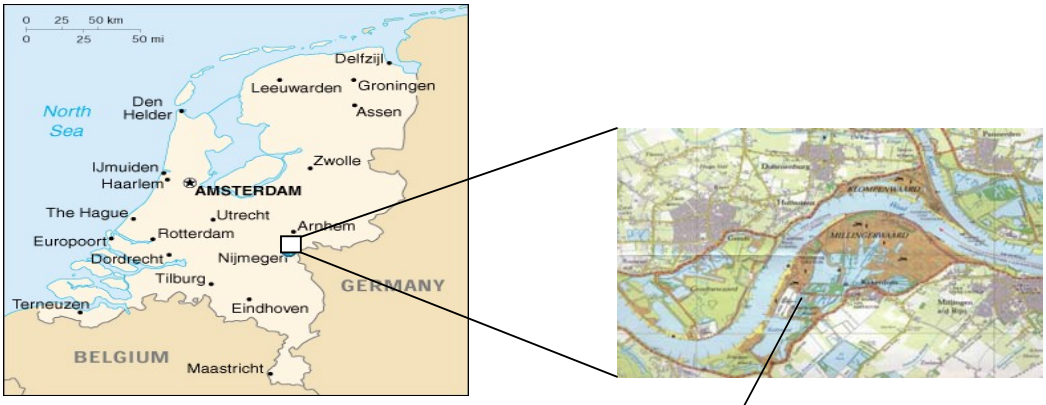

Figure 5: Location of the study area

Figure 6: View of the study area

3.3- Airborne data acquisition

3.3.1- HyMap sensor characteristics

The HyMap sensor is an airborne imaging system that is used for earth resources remote sensing. It records a digital image of the earth's sunlit surface underneath the aircraft but unlike standard aerial cameras, the HyMap records images in a large number of wavelengths. In essence, the HyMap is an airborne spectrometer.

The HyMap records an image of the earth's surface by using a rotating scan mirror which allows the image to build line by line as the aircraft flies forward. The reflected sunlight collected by the scan mirror is then dispersed into different wavelengths by four spectrometers in the system.

For the present study, a single HyMap image is used. The over flight was carried out on July 28th, 2005, over the study area. Additional details on the sensor and image can be found on *Appendix I*.
The input image for this study was already geometrically, radiometrically and atmospherically corrected. Reflectance data per pixel is expressed as [%*100].
For further processing of the airborne data, data outside the study area was masked out, in order to save memory space and computational time.

3.3.2- Quality assessment

Due to the atmospheric conditions on the flight day, only one image was cloud cover free.
After a deep analysis of the quality of the image bands (Kooistra *et al*., 2005) 12 bands have been classified as noisy / bad bands.
Consequently, for the processing of the data in the present study, those bands have been removed and not taken into account, resulting in a 114 bands image.

3.4- Ground data acquisition

3.4.1- ASD measurements for vegetation mapping

Ground data acquisition is indispensable when dealing with remote sensing studies, so that validation of the obtained results can be performed.
Thus, radiometric measurements have been taken in order to asses the atmospheric correction of the images, as well as to validate final results of the study.
These radiometric measurements include reflectance data at the leaf and canopy level.

3.4.2- Leaf ASD measurements

Leaf reflectance spectra were collected on middle August, 2004. For this purpose, the FieldSpec® Pro was used. The obtained spectra have a resolution of 1 nm, over the wavelength range from 350 nm up to 2500 nm.
Around 60 measurements were collected over fresh leaves, half of them using a white background and the remaining half using a black background. Additionally, 5 spectra for each background were collected over the ad – axial side of the leaves, to assist future quality control of the data.
Due to the required time and the amount of data for each species, only the more important ones, from the ecological and spatial point of view, were taken into account in the present study.
To represent the forest area of the Millingerwaard, 3 dominant* forest species were considered. The rest of the study area is represented by 21 dominant species, including low and grassland vegetation.
A detailed description of the measured species can be found in the *Appendix II*.

The collected spectra correspond to the following species:

- *Calamagrostis epigejos*
- *Rubus caesius*
- *Urtica dioica*
- *Populus nigra*
- *Salix fragilis*
- *Salix alba*

** The dominant species have been considered from the ecological and spatial point of view.*

The obtained data was exported as an ASCI II format to perform the pre-process and quality control with Microsoft Excel.
Once the input data was available in Excel, wrong spectra were removed. Water absorption values were removed and an average spectrum was obtained with a spectral resolution of 1nm.
Values of the wavelength range 350 – 399 nm and 2400 – 2500 were removed from the dataset due to its high rate of noise.
Later on, average and standard deviation per band was calculated. Standard deviations were acceptable, for the ab – axial side of the leaves, so no more quality control was needed over the datasets.
With the available data, several spectral libraries were built up, considering separately, for each species: ab - and ad – axial sides of the leaves, and white and black background.

3.4.2.1- Pre-processing of the leaf spectra

Once finished the quality control of the data, reflectance spectra considering white and black background were combined. This step is done due to the assumption that reflectance values are underestimated when using pure black background spectra. So that, new reflectance spectra were calculated according to the expression:

$$\rho = 0.95 * \rho_{bb} + 0.05 * \rho_{wb} \qquad (\textit{Equation 1})$$

where ρ is the measured reflectance value, ρ_{bb} is the measured reflectance value using a black background and ρ_{wb} is the measured reflectance value using a white background.

Later on, Excel data was exported into ASCI II files again. The obtained and corrected spectra were imported into ENVI 4.0 software, to build up referential spectral libraries.

3.4.3- Canopy ASD measurements

A fieldwork campaign took place over the study area on July 28th and August 2nd. For this purpose, the FieldSpec® Pro was used.
Geo-referenced relevees representing the characteristic vegetation communities of the area were selected. For each relevee, 9 canopy reflectance spectra were collected. Additionally, different soil spectra were taken.

The collected spectra have a resolution of 1 nm over the wavelength range from 350 up to 2500 nm. Values of the wavelength range 350 – 399 nm and 2400 – 2500 were removed from the dataset due to its high rate of noise.
White reference spectra were collected also for certain plots, and they were removed from the dataset after assessing the data quality control.
Water absorption bands were also removed for the wavelength range 1350 – 1500 nm and 1760 – 1975 according to Sims (2002), after verifying that these ranges were highly noise for our dataset. To remove the water absorption bands values, the function "Spectral Library Resampling" from ENVI 4.0 software was performed.

Average reflectance spectra and standard deviation per wavelength and relevee were calculated.
Spectral libraries were built up later, to carry out the atmospheric correction of the HyMap images (ATCOR – 4, by VITO agency), for each measured relevee.

3.4.3.1- Pre-processing of the canopy spectra

After performing the quality control of the canopy reflectance spectra, each relevee was characterised by 1 to 3 reflectance measurements. Detailed information about the relevees characterisation can be found in *Appendix III*.
Thus, reflectance measurements corresponding to the same vegetation community (according to Isabel Geloof and Iris de Ronde, 2002) were averaged and assumed to represent the same spatial mixture of vegetation species.

3.5- Radiative Transfer Models

3.5.1- PROSPECT model

The PROSPECT radiative transfer model (Jacquemoud *et al*., 1990) has been employed to describe the vegetation reflectance at foliage level (Fourty, 1996; Jacquemoud *et al*., 1996; Le Maire, 2004). This model accounts for the foliar structure and biochemistry.
The simulated reflectance spectrum ranges from 350 to 2500 μm, with a spectral resolution of 5 μm.

In the model version used for this study, the foliar reflectance depends on 5 parameters: N (foliar structure), C_{ab} (chlorophyll a and b content, in μg/cm^2), C_w (leaf water content, in g/cm^2), C_b (brown pigments content, in μg/cm^2) and C_m (dry mass content, in g/cm^2).

3.5.2- Constraining PROSPECT input parameters

The PROSPECT model was inverted to retrieve biochemical parameters from the ground data spectra, at the foliage level. First guess values were derived from literature review (Hosgood *et al.*, 1995; Grossman *et al*., 1996; Fourty and Baret,1998; Cecatto *et al.*, 2001). Afterwards, 30 model inversions were performed per species to retrieve input values for later simulation. Results of the model inversion can be found on *Table 1*.

To reduce the weight given to the first guesses values, an alpha parameter was implemented on the merit function. This alpha parameter determines the weight that is given to *a priori* values, and was limited to 0.1.
All the model inversion procedure was implemented in Matlab® 7.0 software. The model simulation was run from ENVI / IDL® software.

SPECIES		$(N)_{in}$	$(C_{ab})_{in}$	$(C_w)_{in}$	$(C_m)_{in}$
Calamagrostis epigejos	Maximum	1.40	30	0.010	0.005
	Average	1.40	30	0.008	0.008
	Minimum	1.39	30	0.007	0.001
Populus nigra	Maximum	2.00	95	0.017	0.006
	Average	1.95	95	0.015	0.005
	Minimum	1.9	95	0.013	0.004
Rubus caesius	Maximum	1.50	75	0.011	0.009
	Average	1.50	75	0.010	0.005
	Minimum	1.49	75	0.008	0.002
Salix alba	Maximum	1.95	90	0.015	0.010
	Average	1.9	90	0.015	0.010
	Minimum	1.85	90	0.010	0.010
Salix fragilis	Maximum	1.95	90	0.015	0.010
	Average	1.9	90	0.010	0.010
	Minimum	1.85	90	0.010	0.005
Urtica dioica	Maximum	1.50	71	0.010	0.003
	Average	1.50	71	0.008	0.002
	Minimum	1.49	71	0.007	0.001

Table 1: PROSPECT parameters ranges retrieved from model inversion

Due to the lower influence of the brown pigments in the construction of the model (Fourty et al., 1996), this parameter has not been taken into account for the model inversion. However, the model simulation will account for them, so average ranges were estimated from literature review (Hosgood *et al*., 1995).

Then, PROSPECT simulation was performed. Simulation ranges used for the PROSPECT model and based on the model inversion results are specified on *Table 2*. Later on, spectral libraries of the leaf reflectance per species were built. Finally, modelled leaf reflectance spectra were used as an input for the SAIL model.
For the rest of the species, average range for the parameters' intervals were calculated, to model the required spectra (*Table 2*), assuming to be present 2 different vegetation groups (*Agrostis stolonifera**, *Cirsium arvense**).

Species	$(N)_M$	$(C_{ab})_M$	$(C_w)_M$	$(C_m)_M$	$(C_b)_M$
Calamagrostis epigejos	1.39 – 1.40	30	0.010 – 0.008 – 0.007	0.005 – 0.003 – 0.001	0.05
Populus nigra	1.90 – 1.95	95	0.013 – 0.015 – 0.017	0.004 – 0.005 – 0.006	0.05
Rubus caesius	1.49 – 1.50	75	0.011 – 0.010 – 0.008	0.009 – 0.005 – 0.002	0.10
Salix alba	1.85 – 1.95	90	0.010 – 0.015	0.010	0.05
Salix fragilis	1.85 – 1.95	90	0.010 – 0.015	0.010 – 0.005	0.05
Urtica dioica	1.49 – 1.50	71	0.010 – 0.008 – 0.007	0.003 – 0.002 – 0.001	0.10
Agrostis stolonifera*	1.40	30	0.005	0.005	0.05
Cirsium arvense*	1.55	71	0.015	0.002	0.10

Table 2: PROSPECT model parameters: simulation ranges

** Unmeasured species have been assumed to have different spectral properties according to its leaf and plant structure. The 2 different types of vegetation correspond to:*

1) *Agrostis stolonifera, Poa triviales, Arrhenatherum elatius, Carex hirta, Cynodon dactylon, Elymus repens, Festuca rubra, Lolium perenne*
2) *Cirsium arvense, Eryngium campestre, Euphorbia cyparissias, Euphorbia esula, Medicago falcata, Potentilla reptans, Ranunculus repens, Senecio jacobaea, Tanacetum vulgare, Trifolium repens*

3.5.3- SAIL model

The SAIL radiative transfer model (Verhoef, 1984) is widespread in the remote sensing community for the estimation of vegetation biophysical variables. It calculates the canopy reflectance, from the leaf optical properties and a limited number of variables describing its architecture: The leaf area index *LAI*, the mean leaf inclination angle *ALA*, assuming an ellipsoidal distribution of foliage elements (Campbell, 1990), the hot spot parameter s_l, the view zenith angle, the sun zenith angle (rad), the relative azimuth angle, view - sun (rad) and the diffuse fraction.

To perform the simulation, not only biophysical variables to describe the canopy structure, but also soil background and foliage level spectra have to be defined as input parameters.

3.5.4- Constraining SAIL input parameters

The simulated spectra from the PROSPECT model were used, considering 3 input spectra for each of the 6 species from which field spectra was available and 1 input spectrum for the rest of the species.
Due to the characteristics of the study area, an agricultural bare soil was chosen as background. Its reflectance spectrum has been taken from a HyMap image of the study area.
From the geological point of view, it would have clay and sand radiometric properties. However, due to the characteristics of the vegetation area, only the upper horizon (organic matter) has been considered. This soil can be considered as a dark one, with a composite estimation of: 10 % clay, 10% sand, 80 % organic matter.

The required parameter's ranges were estimated from previous scientific studies (Sellers et al., 1996). For the illumination conditions atmospheric correction parameters used for the HyMap images (ATCOR – 4) were considered as an input for the model. Only one illumination condition was taken into account, corresponding to the day of the flight for the HyMap image.
The used parameters' ranges are specified in *Table 3*.

Species	Type of Veg. (I)	Type of Veg. (II)	LAI	ALA	HS parameter	V. ZENITH ANGLE	SUN ZENITH ANGLE	AZIMUTH ANGLE
Agrostis stolonifera	Graminoid	Grassland	0.3 - 5	5 – 60	0.0125	0º	32.9º	0º
Arrhenatherum elatius	Graminoid	Grassland	0.3 - 5	5 – 60	0.0125	0º	32.9º	0º
Calamagrostis epigejos	Graminoid	Grassland	0.3 - 5	5 – 60	0.0125	0º	32.9º	0º
Carex hirta	Graminoid	Grassland	0.3 - 5	5 – 60	0.0125	0º	32.9º	0º
Cirsium arvense	Forb-herb	Grassland	0.3 - 5	5 – 60	0.0125	0º	32.9º	0º
Cralaegus monogyna	Forb-herb	Grassland	0.3 - 5	5 – 60	0.0125	0º	32.9º	0º
Cynodon dactylon	Graminoid	Grassland	0.3 - 5	5 – 60	0.0125	0º	32.9º	0º
Elymus repens	Graminoid	Grassland	0.3 - 5	5 – 60	0.0125	0º	32.9º	0º
Eryngium campestre	Forb-herb	Grassland	0.3 - 5	5 – 60	0.0125	0º	32.9º	0º
Euphorbia cyparissias	Forb-herb	Grassland	0.3 - 5	5 – 60	0.0125	0º	32.9º	0º
Euphorbia esula	Forb-herb	Grassland	0.3 - 5	5 – 60	0.0125	0º	32.9º	0º
Festuca rubra	Graminoid	Grassland	0.3 - 5	5 – 60	0.0125	0º	32.9º	0º
Lolium perenne	Graminoid	Grassland	0.3 - 5	5 – 60	0.0125	0º	32.9º	0º
Medicago falcata	Forb-herb	Grassland	0.3 - 5	5 – 60	0.0125	0º	32.9º	0º
Poa trivialis	Graminoid	Grassland	0.3 - 5	5 – 60	0.0125	0º	32.9º	0º
Populus nigra	Tree	Dec. Forest	1.6 - 8.8	20 - 75	0.00400	0º	32.9º	0º
Potentilla reptans	Forb-herb	Grassland	0.3 - 5	5 - 60	0.0125	0º	32.9º	0º
Ranunculus repens	Forb-herb	Grassland	0.3 - 5	5 - 60	0.0125	0º	32.9º	0º
Rubus caesius	Shrub	Open shrub land	1.6 -4.5	20 - 75	0.00319	0º	32.9º	0º
Salix alba	Tree	Dec. Forest	1.6 - 8.8	20 - 75	0.00400	0º	32.9º	0º
Salix fragilis	Tree	Dec. Forest	1.6 - 8.8	20 - 75	0.00400	0º	32.9º	0º
Senecio jacobaea	Forb-herb	Grassland	0.3 - 5	5 - 60	0.0125	0º	32.9º	0º
Tanacetum vulgare	Forb-herb	Grassland	0.3 - 5	5 - 60	0.0125	0º	32.9º	0º
Trifolium repens	Forb-herb	Grassland	0.3 - 5	5 - 60	0.0125	0º	32.9º	0º
Urtica dioica	Forb-herb	Grassland	0.3 - 5	5 - 60	0.0125	0º	32.9º	0º

Table 3: SAIL model parameters: simulation ranges

3.5.4.1- SAIL parameters:

In order to simplify the model simulation, different radiometric scenarios have been defined, according to the type of species.
3 different cases have been distinguished to represent the vegetation variability of the study area. The used simulation ranges for the SAIL model are specified in *Tables 4 - 6.* Additionally, each corresponding scenario per specie has been modelled for each of the 3 PROSPECT spectra named previously as an input.
Thus, as a result, 8 different spectral libraries have been built up, 6 for each of the measured species and 2 for the general types of vegetation. Each spectral library contains the following number of spectra: 72 canopy reflectance spectra for each of the 6 measured species and 24 canopy reflectance spectra for the rest of the species.

3.5.4.2- Radiometric scenarios:

a- **Grassland:** ***Calamagrostis epigejos, Urtica dioica***

Parameter	***Level (s)***
Leaf area index	0.3, 1, 2, 3, 4, 5
Average leaf angle	5, 20, 35, 50
Hot spot parameter	0.0125
View zenith angle	0
Sun zenith angle (rad)	0.574
Rel azimuth angle, view - sun (rad)	0
Diffuse fraction	0

Table 4: SAIL parameter levels / Radiometric Scenarios (Schaepman et al., 2002)

b- **Open Shrub land:** ***Rubus caesius***

Parameter	***Level (s)***
Leaf area index	0.3, 1, 2, 3, 4, 5
Average leaf angle	5, 20, 35, 50
Hot spot parameter	0.006
View zenith angle	0
Sun zenith angle (rad)	0.574
Rel azimuth angle, view - sun (rad)	0
Diffuse fraction	0

Table 5: SAIL parameter levels / Radiometric Scenarios (Schaepman et al., 2002)

c- **Deciduous Forest:** ***Populus nigra, Salix alba, Salix fragilis***

Parameter	***Level (s)***
Leaf area index	1.6, 3, 4.5, 6, 7.5, 8.8
Average leaf angle	20, 35, 50, 65, 75
Hot spot parameter	0.004
View zenith angle	0
Sun zenith angle (rad)	0.574
Rel azimuth angle, view - sun (rad)	0
Diffuse fraction	0

Table 6: SAIL parameters levels / Radiometric Scenarios (Schaepman et al., 2002)

Note**:** for the unmeasured species, the "grassland radiometric scenario" has been applied, considering the corresponding "type of vegetation".

3.6- Linear Spectral Unmixing

Linear spectral mixture analysis is a technique that has been widely used in vegetation studies (Borel and Gerstl, 1994; Garcia-Haro *et al*., 1996; Gilabert *et al*., 2000; Underwood *et al*., 2003). It consists on determining the amount of a certain materials, within a pixel, in terms on contribution to the spectral features.
In the present study, this technique is applied at 2 different levels. First, it is used to determine spectral contribution of a certain species within each pixel of the image, in terms of reflectance. Secondly, the vegetation community spectral reflectance is modelled to retrieve the average LAI of each species for the study area, and to detect certain species associations in the study area, from remote sensing data.
Linear spectral unmixing can be applied using several constrains, or none of them. Two cases are compared in this study, named Unconstrained Linear Spectral Unmixing (ULSU) and Fully Constrained Linear Spectral Unmixing (FCLSU).

3.6.1- Unconstrained Linear Spectral Unmixing

Unconstrained Linear Spectral Unmixing (ULSU) is a procedure that consists on solving several linear equations in the form (Heinz C. and Chang C., 2001):

$$r = M\alpha + n \qquad (\textit{Equation 2})$$

where r is the pixel value in a hyperspectral image, M is the material signature, α is the material abundance and n is the noise or measurement error.

In this form, negative as well as above one values are considered as possible solutions. The justification of this technique relies on the assumption of the presence of unknown materials. Thus, the reflectance of each pixel in the image corresponds to a linear combination of abundance of each defined material (called endmembers), plus the contribution of unknown materials reflectance.

3.6.1.1- Vegetation parameter retrieval:

Reflectance spectra for each species were available as a combination of different parameters, as an output from the SAIL model. However, only one spectrum (endmember) per species can be used in the ULSU procedure, with the purpose of retrieving spatial abundance values of each endmember per pixel.
Then, knowing that the LAI parameter is the one that most influences the reflectance spectrum at the canopy level within the SAIL model, an average value for it had to be chosen for the whole study area.

So as to, the LAI map distribution for the study area was used, from Mengesha, 2005.
The ground data relevees were located in the LAI map and then, LAI values were determined for each location. Additionally, spatial coverage per species in each of the

relevees is known (*Appendix IV*). Thus, the relevee LAI can be assumed to be an addition of the LAI value of each species present per relevee.
To retrieve the average LAI value for each considered species, the 3 more extent ones per vegetation community were chosen. Then, each vegetation community was assumed to have the reflectance spectrum resulted from the combination of 3 pure reflectance spectra.
However, there were several combinations of spectra that could give the additive LAI value for the vegetation community. All the possible mixtures of 3 species, per vegetation community that fulfil this requirement (additive LAI value) were simulated.

The simulated mixed spectra were compared with the ground data spectra collected at the canopy level. This ground data spectra were located in each measured relevee, thus, spatial coverage of the species and corresponding vegetation community is known. When more than one ground canopy spectra was available for the same vegetation community (different relevees corresponding to the same vegetation community or species mixture), spectra were averaged.
When comparing simulated spectra with ground data spectra, both for vegetation communities and canopy reflectance, the simulated spectra having the higher correlation was chosen.
Thus, the chosen spectra correspond to a certain species mixtures, where each species is characterised by an average LAI value.
The retrieved LAI value per specie was assumed to be the average one for the whole study area.
Nevertheless, certain species were present in different vegetation communities. In those cases, were more than one average LAI value was supposed, the average one was determined to be the retrieved for the vegetation community that covers more area within the test site.

The obtained correlation between simulated and measured spectra for each of the vegetation communities are shown in *Appendix V*.
As an example, correlation found for vegetation community 15 (RG van *Rubus caesius* [*Galio-Urticetea*]) is represented in *Figure 7*.

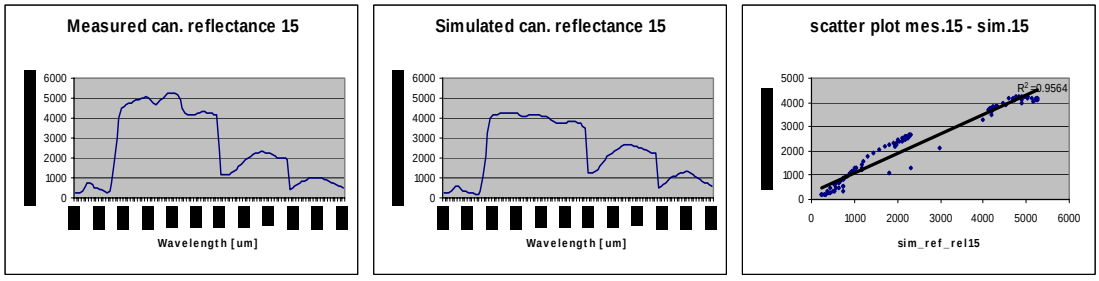

Figure 7: Correlation between simulated and measured spectra for vegetation community 15.

3.6.1.2- Species level

Once determined the average LAI spectra per species for the study area, Linear Spectral Unmixing at the species level could be applied.

In order to optimise the results, different combinations of endmembers have been tried out. The present species of the area have been ordered by means of spatial coverage. Later on, assuming the water and soil spectra to contribute in all the cases, the ULSU have been performed with one species, 2, 3, and so on. Obtained results have been systematically compared, for each case, with the existing vegetation map of the area.

3.6.1.3- Vegetation communities

After completing the simulation of the vegetation community spectra, the vegetation communities were ordered by means of correlation between simulated and measured spectra. Later on, following the same procedure of the species level case, ULSU as a combination of different endmembers was computed. The difference in this case is that the LSU was applied not to the whole study area, but per each of the considered vegetation communities' areas as defined by Isabel Geloof and Iris de Ronde, 2002. As in the previous case, assuming that not all the vegetation communities are represented, soil and water reflectance spectra were considered as fixed endmembers.
Additionally, reflectance spectra per vegetation community where derived from the HyMap image. Thus, the results (Chapter 4) are presented as 3 different approaches: simulated spectra, ground data canopy spectra and image reflectance spectra.

3.6.2- Fully Constrained Linear Spectral Unmixing

Fully Constrained Linear Spectral Unmixing (FCLSU) is based in the same principle as equation (2). However, in this case, 2 constrains are imposed on the linear mixture model: the abundance sum-to-one constrain and the abundance non-negativity constrain, mathematically expressed in the form (Heinz and Chang, 2001):

1) sum to one constrain:

$$\Sigma^{p}_{j=1}\ \alpha_j = 1 \qquad (\textit{Equation 3})$$

2) abundance non negativity constrain:

$$\alpha_j = 1 \text{ for all } 1 \leq j \leq p \qquad (\textit{Equation 4})$$

where α_j is the abundance fractions of the materials present in the scene and p is the number of material signatures.

Notice that in this case the assumption of fully representation of the study area with the used endmembers is indirectly done.

3.6.2.1- Species level

FCLSU has been implemented in Matlab® 7.0, as this procedure is not available in IDL/ENVI®. The use endmembers are the ones that resulted to give better results for the ULSU case.
The obtained results were later on compared with the ULSU case. Results are discussed in chapter 4.

4- RESULTS AND DISCUSSION

4.1- Spectral libraries

4.1.1- PROSPECT spectral libraries

Spectral libraries for reflectance spectra at the leaf level have been built up. These data includes the simulated reflectance using the PROSPECT model, for each considered species.
In relation with the conceptual model of the study, it corresponds to the output obtained at the leaf level, represented as Lρ for the 'model' case.

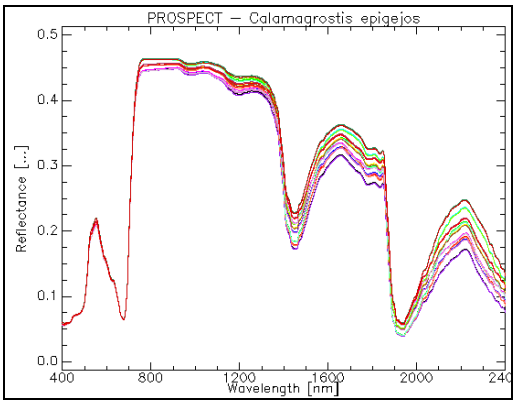

Figure 8: Simulated spectra with PROSPECT model for Calamagrostis epigejos

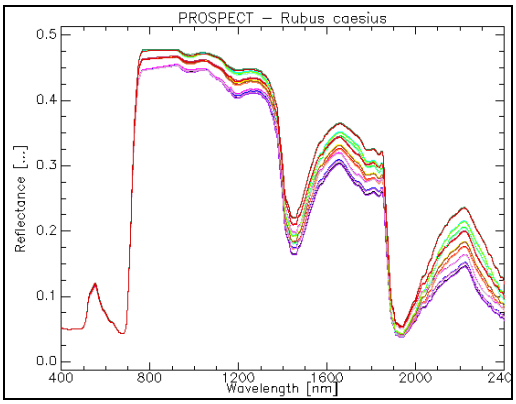

Figure 9: Simulated spectra with PROSPECT model for Rubus caesius

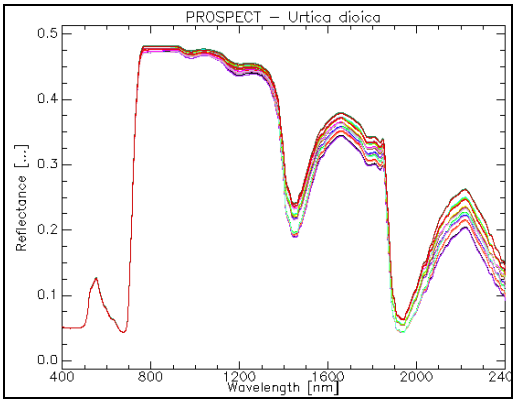

Figure 10: Simulated spectra with PROSPECT model for Urtica dioica

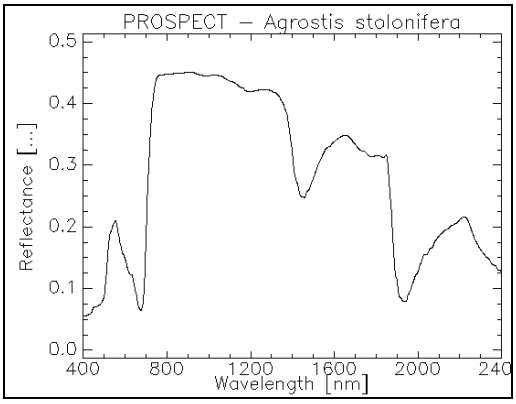

Figure 11: Simulated spectra with PROSPECT model for Agrostis stolonifera

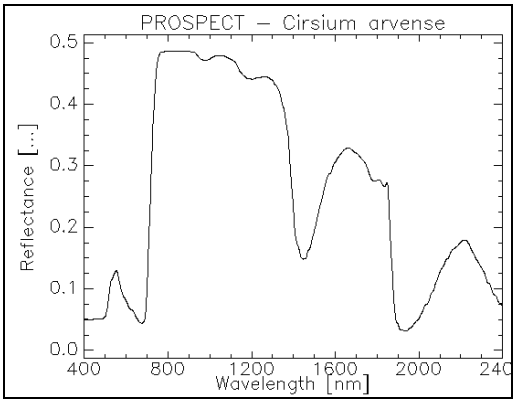

Figure 12: Simulated spectra with PROSPECT model for Cirsium arvense

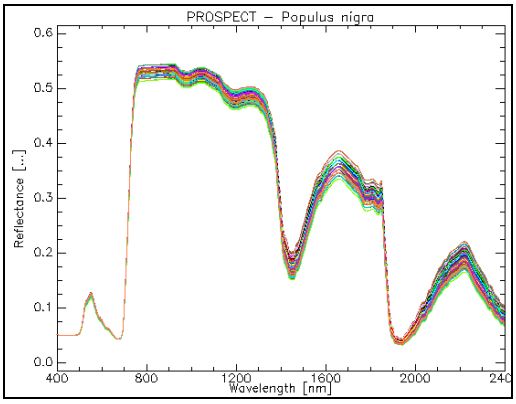

Figure 13: Simulated spectra with PROSPECT model for Populus nigra

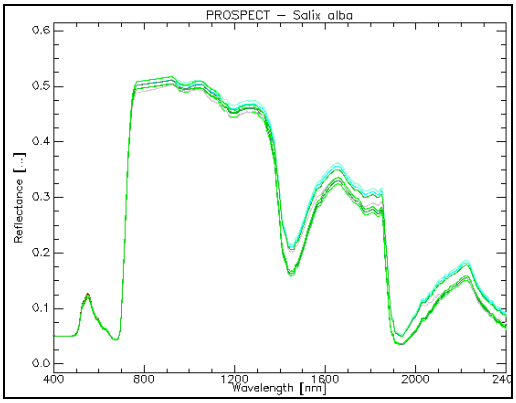

Figure 14: Simulated spectra with PROSPECT model for Salix alba

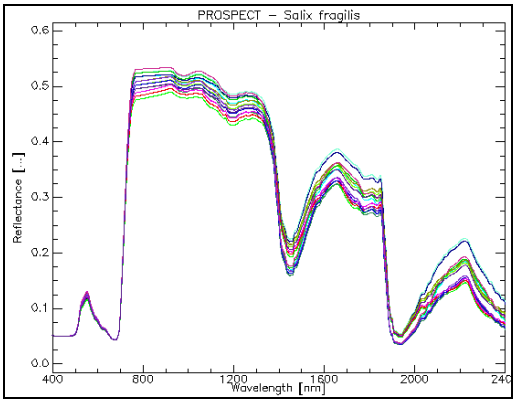

Figure 15: Simulated spectra with PROSPECT model for Salix fragilis

4.1.1.1- Grassland - shrub land species

Variations observed in the spectral libraries (*Figures 8-12*) are due to the modelled ranges for each parameter and species. Different chlorophyll contents can be noticed in the blue, green and red part of the spectrum, corresponding to the 400 – 700 nm. plateau. As observed in the case for *Calamagrostis epigejos*, the reflectance peak in the green part is higher. This fact is due to the lower content of chlorophyll in this specie. Contrarily to it, *Rubus caesius* and *Urtica dioica* have higher chlorophyll content, which is demonstrated by the lower reflectance (higher absorption) values at wavelengths corresponding to the 400 – 700 nm.

Additionally, differences between species can be appreciated in the NIR part of the spectrum. Species with a higher N value for the PROSPECT model show a higher reflectance. This is explained by the influence of the leaf structure over the NIR wavelengths. In accordance with previous studies, monocotyledonous species (*Calamagrostis epigejos*) show a lower reflectance than species with a dicotyledonous structure (*Rubus caesius, Urtica dioica*). Also in this wavelength range, the influence of the dry mass content (C_b) is demonstrated.

From the spectral libraries, wider variation range within the modelled spectra appears for *Rubus caesius*. The difference between spectra is explained by the modelled ranges for the C_b parameter. *Rubus caesius* retrieved range from the model inversion was wider. Thus, differences in the NIR part of the spectrum for the modelled cases are higher than for *Calamagrostis epigejos* or *Urtica dioica*.

Leaf water content has a great influence on the reflectance spectra, due to the optical properties of the water molecule. In the present case, this characterise can be perceived on the 900 – 2500 wavelength range. C_w determines the stronger absorption observable in the *Rubus caesius* spectra, around 1400 nm. It also contributes to the lower reflectance peak on the 2100 – 2300 nm. range. When comparing these spectra with the ones for *Calamagrostis epigejos* and *Urtica dioica*, the last ones present higher reflectance values for this wavelength range. From the modelled parameters' intervals we clearly see that the simulated water content is lower, and it consequently influences on the spectral properties of the species.

Observed differences between *Agrostis stolonifera* and *Cirsium arvense* reflectance spectra summarize the different spectral properties between monocotyledonous and dicotyledonous species.

4.1.1.2- Forest species

The three forest species show similar reflectance rates for the reflectance peaks within the 400 – 2400 range of the spectrum.

Concerning the 400 – 700 nm. range, no sharp differences are found, due to the similar chlorophyll content in the leaves. Reflectance values at the NIR part are also similar, with only slightly differences over the absorption deep located around 1200 nm. This difference could be used to distinguish between the three species. This absorption peak is related to leaf structure and dry matter content. Considering that the N value (leaf structure) for the three species is similar, the deep can be assumed to be a consequence of the dry biomass content. *Salix alba* and *Salix fragilis* present stronger absorption at this wavelength than *Populus nigra*, as its dry matter content within the leaves is lower.

For the 1500 – 2500 nm. range, water content, leaf structure and dry matter content are the main responsible observed variations. *Populus nigra* modelled spectra appear in continuous intervals. This characterise is explained by the narrow modelling interval for C_w and C_m parameters. *Salix alba* spectra appear to be in 2 main groups according to the reflectance values within this range. The 2 groups are a consequence of the possible combinations of modelled values for Cw and Cm.
Finally, the same grouping phenomenon as for *Salix alba* is observed for *Salix fragilis*, with the difference that spectra appear as 3 main groups. Regarding the model parameters ranges for Cw and Cm for this specie, similar conclusion can be drawn.

4.1.2- SAIL spectral libraries

Spectral libraries for reflectance spectra at the canopy level have been built up. These data includes the simulated reflectance using the SAIL model, for each considered species. They show a wide range of variation, mainly due to the modelled *LAI* and *ALA* ranges.

In relation with the conceptual model of the study, it corresponds to the output obtained at the canopy level, represented as Cρ for the 'model' case.

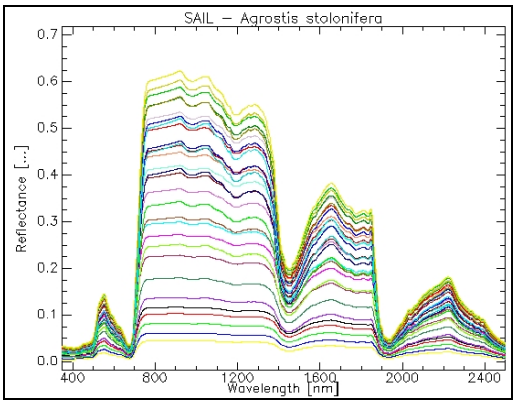

Figure 16: Simulated spectra with SAIL model for Agrostis stolonifera

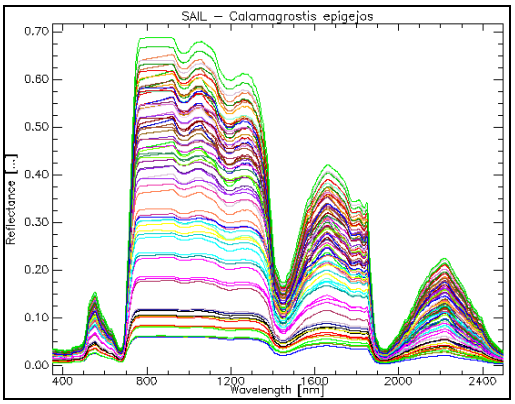

Figure 17: Simulated spectra with SAIL model for Calamagrostis epigejos

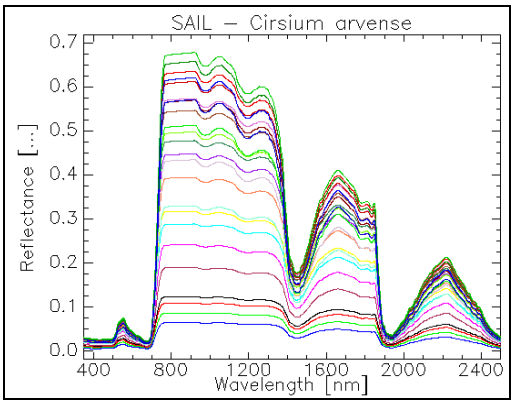

Figure 18: Simulated spectra with SAIL model for Cirsium arvense

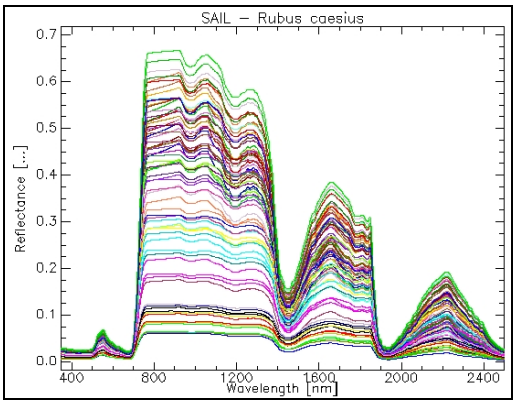

Figure 19: Simulated spectra with SAIL model for Rubus caesius

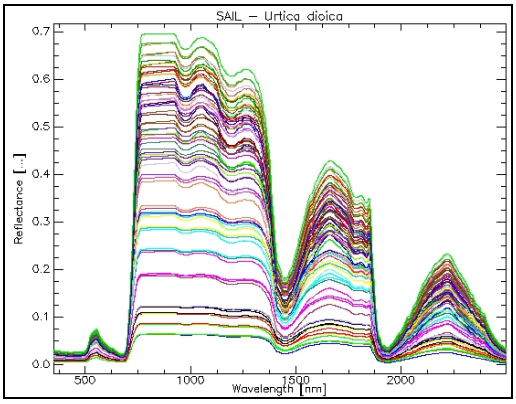

Figure 20: Simulated spectra with SAIL model for Urtica dioica

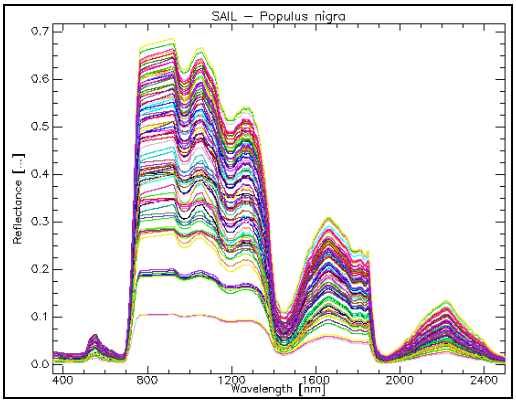

Figure 21: Simulated spectra with SAIL model for Populus nigra

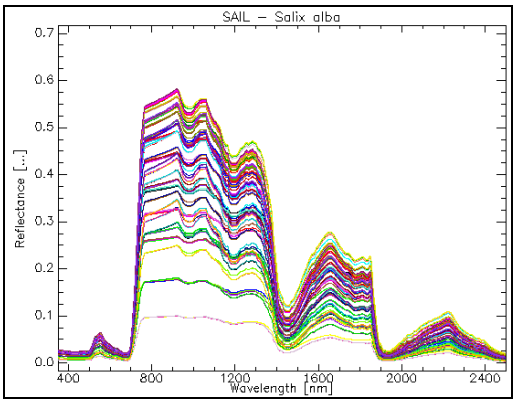

Figure 22: Simulated spectra with SAIL model for Salix alba

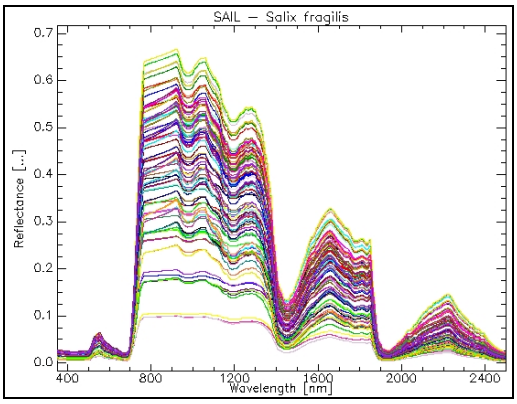

Figure 23: Simulated spectra with SAIL model for Salix fragilis

4.1.2.1- Grassland – shrub land species

SAIL spectral libraries (*Figures 16-20*) correspond to the canopy reflectance spectra. Due to the soil background contribution and multiple scattering between different leaves, the reflectance is higher. As well as in the leaf reflectance case, biochemical compounds have a great influence on the reflectance spectra. For the *Rubus caesius*, *Cirsium arvense* and *Urtica dioica* case, the reflectance over the 400 – 700 nm. range is lower than for the *Agrostis stolonifera* and *Calamagrostis epigejos* species, due to the higher chlorophyll content. Following the same reasoning line, reflectance values over the NIR part of the spectrum can be explained. The main observed difference appears again between monocotyledonous (*Calamagrostis epigejos, Agrostis stolonifera*) and dicotyledonous (*Cirsium arvense, Rubus caesius, Urtica dioica*) species. The last ones show a higher reflectance. However, the leaf structure influence is not as high as for the leaf reflectance case.

For the canopy case, the observed variations over the NIR part of the spectrum are explained by the different LAI and ALA modelled ranges. For each spectral library,

higher LAI values result in higher reflectance values, and the opposite is true for the ALA parameter.

The modelled ranges are very wide, but all the possible cases wanted to be represented in this study, so very different LAI and ALA values had to be modelled.
However, not all the modelled spectra will be used. Only the corresponding to retrieve LAI average values (see next sections) will be taken into account.

Observed differences between *Agrostis stolonifera* and *Cirsium arvense* reflectance spectra summarize the different spectral properties between monocotyledonous and dicotyledonous species.

4.1.2.2- Forest species

Chlorophyll content at the canopy level for the three forest species is similar, according to reflectance peak and absorption deeps observed within the 400 – 700 nm. range.

Concerning the reflectance values in the NIR part of the spectrum, *Salix alba* presents marked differences with *Salix fragilis* and *Populus nigra*. The lower reflectance values observed for *Salix alba* are due to the higher dry matter content in the leaves. This feature was not so clear at the leaf level spectra. However, when considering the canopy level, more leaves are taken into account. So that, absorption features due to dry biomass content appear enhanced. This specific feature is also observable when comparing reflectance values for wavelength above 2000 nm.

As in the previous cases (grassland – shrub land species), the wide reflectance variation between modelled spectra for all the three species is explained by the modelled LAI and ALA parameters.

Comparing the forest species with the grassland and shrub land species, higher reflectance values are appreciate across all the wavelengths, due to the higher modelled values for the LAI parameter.

4.2- PROSPECT parameter retrieval

PROSPECT parameters have been retrieved by means of model inversion. Matlab® software was used to perform this step, minimising the Root Mean Square error (RMS) between the simulated and measured spectra.

As a result, maximum, minimum and average values for the constrained parameters were obtained. Only the N, C_{ab}, C_w and C_m were inverted. C_b was not taken into account due to its low influence (Fourty *et al*., 1996) on the reflectance spectra as a parameter in PROSPECT model.
Illness possessed cases were obtained for certain number of inversions. However, due to the large amount of measured data, they were not considered a determine pitfall of the procedure.

Table 7 shows the obtained parameters' ranges for the measured species.

Species	$(N)_M$	$(C_{ab})_M$	$(C_w)_M$	$(C_m)_M$	$(C_b)_M$
Calamagrostis epigejos	1.40 – 1.39	30	0.010 – 0.007	0.005 – 0.001	0.05
Populus nigra	1.95 – 1.90	95	0.017 – 0.013	0.006 – 0.004	0.05
Rubus caesius	1.50 – 1.49	75	0.011 – 0.008	0.009 – 0.002	0.10
Salix alba	1.95 – 1.85	90	0.015 – 0.010	0.010	0.05
Salix fragilis	1.95 – 1.85	90	0.015 – 0.010	0.010 – 0.005	0.05
Urtica dioica	1.50 – 1.49	71	0.010 – 0.007	0.003 – 0.001	0.10
Agrostis stolonifera	1.40	30	0.005	0.005	0.05
Cirsium arvense	1.55	71	0.015	0.002	0.10

Table 7: Retrieved parameters' ranges for the PROSPECT model inversion

Retrieved ranges from the PROSPECT parameters describe the biochemical properties of each species.
As expected, *Calamagrostis epigejos* and *Agrostis stolonifera* have an N value bellow 1.5, which is characteristic for monocotyledonous species. For the rest of the species (dicotyledonous), N values are above 1.5. Forest species (*Salix alba, Salix fragilis* and *Populus nigra*) have a higher N value than grassland and shrub land species (*Cirsium arvense, Rubus caesius* and *Urtica dioica*). This is due to the different structure of the leaves.
Chlorophyll contents are lower for grasses (*Calamagrostis epigejos* and *Agrostis stolonifera*) than for the rest of the species.
Leaf water and dry biomass content, in general, is higher for forest species.
In general, the obtained results match well with the ranges found in literature. However, grassland species parameters vary widely with the specific conditions of the study area, thus, model inversion is highly recommended to retrieve the PROSPECT parameters. On the other hand, forest species have been widely studied and documented in previous studies and the obtained values for the biochemical parameters are in accordance with those reported in literature.

4.3- Biophysical parameter retrieval: Leaf Area Index

Mixed species spectra for the different communities have been simulated, according to its spatial coverage over the study area and relevee location.
Thus, LAI could be retrieved for certain species (the more spatially abundant ones). Results and correlation between reflectance spectra of the investigated species* are presented in *Tables 8 and 9*.
The procedure to reach these results was explained in the previous chapter.

	Calamagrostis epigejos	*Carex hirta**	*Dactylis glomerata**	*Phleum pratense**	*Rumex acetosa**	*Rubus caesius*	*Urtica dioica*	*Epilobium tetragonum**	*Cirsium arvense**
Average LAI	1	1	2	3	1	2	2	2	3
	Monocotyledonous				Dicotyledonous				
	→ LAI				→ LAI				

Table 8: Average LAI value for the study area per specie.

LAI values for the present study area resulted to be overestimated in the literature, according to the modelled ranges. However, it is possible (and occurs for some of the cases) that higher or lower values that the ones cited here appear in the test site.

Due to the aim of performing linear spectral unmixing for the whole study area and using different reflectance spectra per specie, an average spectrum had to be chosen. So that, the election was done according to the following criteria: spatial coverage, LAI value, biochemical properties (mainly leaf structural parameter), ecological dominance and vegetation type (monocotyledonous vs. dicotyledonous). The cited determinant parameters have shown a good differentiation over different species. From the retrieved results, it can be seen that, in general, grasslands and shrub land species have a LAI value between 1 and 3, in its average form. Anyway, as settle before, higher or lower values may be possible due to specific variations between single plants and growing conditions.

** The following groups of species have been assumed have similar spectral properties (according to leaf structure and LAI value):*

- *Carex hirta, Cynodon dactylon, Festuca rubra*
- *Dactylis glomerata, Elymus repens, Lolium perenne*
- *Phleum pratense, Poa annua*
- *Rumex acetosa, Senecio inaequidens*
- *Epilobium tetragonum, Eryngium campestre, Mentha aquatica, Potentilla reptans, Trifolium repens*
- *Cirsium arvense, Glechoma hederacea, Lythrum salicaria*

	Calamagrostis epigejos	*Carex hirta**	*Dactylis glomerata**	*Phleum pratense**	*Rumex acetosa**	*Rubus caesius*	*Urtica dioica*	*Epilobium tetragonum**	*Cirsium arvense**
Calamagrostis epigejos	1	0.9993	0.9985	0.9943	0.9692	0.9833	0.9795	0.9755	0.9761
*Carex hirta**		1	0.9974	0.9917	0.9748	0.9827	0.9814	0.9787	0.9773
*Dactylis glomerata**			1	0.9983	0.9719	0.9911	0.9856	0.9810	0.9838
*Phleum pratense**				1	0.9649	0.9938	0.9843	0.9781	0.9843
Rumex acetosa					1	0.9781	0.9931	0.9966	0.9893
Rubus caesius						1	0.9947	0.9907	0.9963
Urtica dioica							1	0.9993	0.9993
*Epilobium tetragonum**								1	0.9979
*Cirsium arvense**									1
	Monocotyledonous				Dicotyledonous				
	→ LAI				→ LAI				

Table 9: Correlations between simulated reflectance spectra per specie.

The correlation values presented above can be analysed from different points of view.

Regarding the monocotyledonous species (upper-left side of the table), similarity between reflectance spectra decreases as the LAI values differ more from each other. Thus, species with similar LAI values have more similar spectral properties.
In the case that concerns, this property is enhanced by the fact that there is no wide variation over this parameter for the studied species. Focussing on the lower-right side of the table, correlations between dicotyledonous species are presented. Highly correlated reflectance spectra appear for those species with moderate to high LAI values. When the LAI is higher, more correlation between species with similar value is observed.

Comparison between monocotyledonous and dicotyledonous species is represented by the values located on the upper – right side of the table. There is a clear difference between monocotyledonous and dicotyledonous species, as was demonstrated previously.

However, spectral properties for monocotyledonous species with middle to high LAI correlate with the dicotyledonous ones with similar LAI. Thus, for this kind of species (grassland and shrub land) and LAI ranges (1 to 3), spatial attention should be put when interpreting the results, as there is a possibility for species with similar LAI value to be mistaken. The reason for this statement is that LAI parameter has a great influence on the reflectance rate, thus biochemical and other biophysical properties characterising each species could be masked out.

4.4- Abundance maps

4.4.1- Species level

4.4.1.1- Unconstrained Linear Spectral Unmixing

Best results were obtained when using 6 reflectance spectra at the species level. Additionally, due to the wide considered area used for the unmixing procedure, soil and water spectra were also included as endmembers in the procedure.
This operation has been performed in two different software', ENVI / IDL® and MATLAB®. They use a different approach for the error calculation (LaGrange multipliers vs. Newton series). However, obtained results do not show sharp differences. So the use of ENVI / IDL® or MATLAB® does not influence the results for the ULSU procedure.
The considered species were chosen by means of spatial coverage over the whole study area. Thus, the obtained abundance maps (*Figure 26 - 31*) represent the more abundant species, by means of spatial coverage, within the study area.

All the presented maps are referred to the base image shown in *Figure 24*. They have the same reference system and scale.

Figure 24: Base map: true colour HyMap image of the study area.

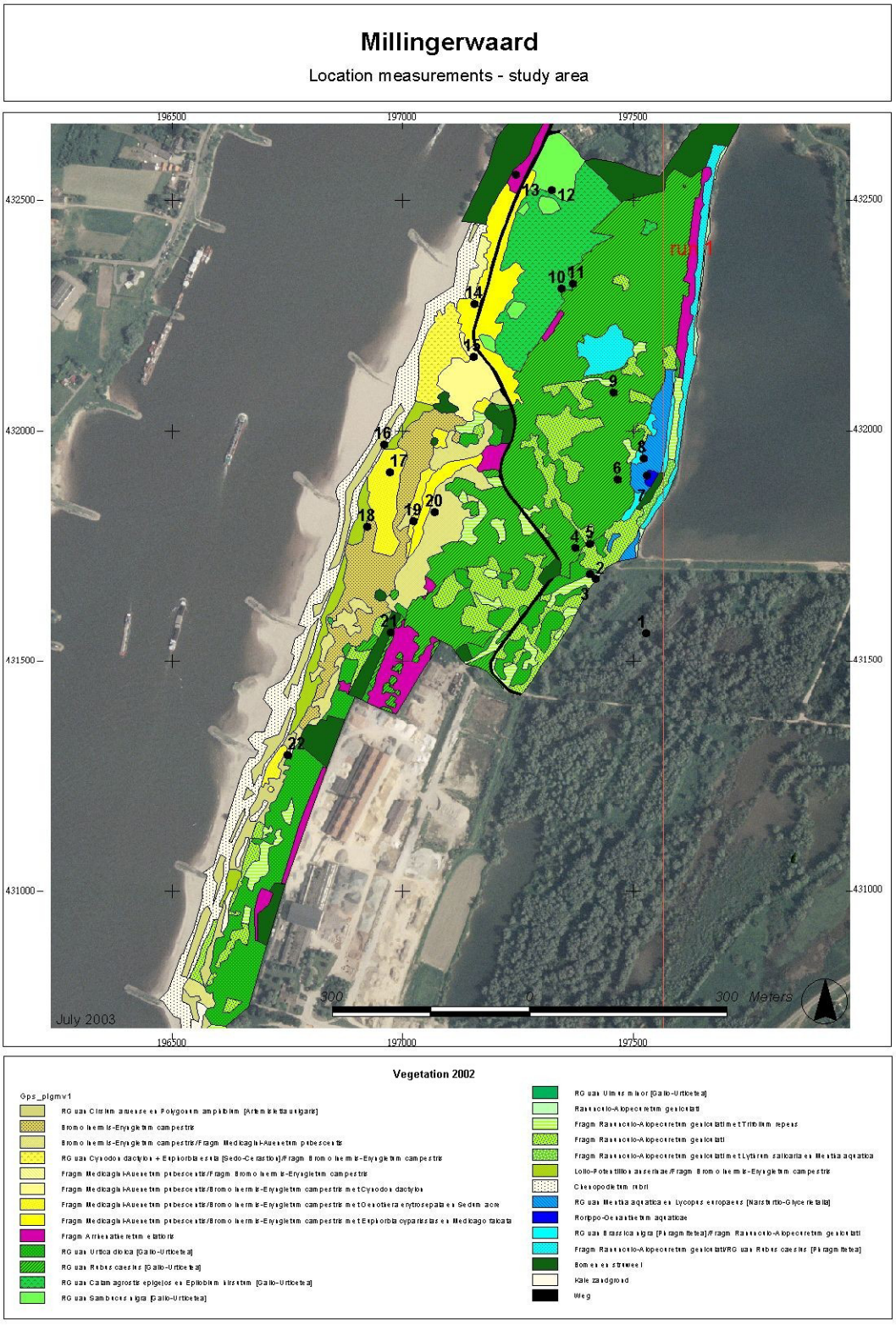

Figure 25: Vegetation map for the study area (Geloof and de Ronde, 2002)

4.4.1.1.1- Unconstrained Linear Spectral Unmixing

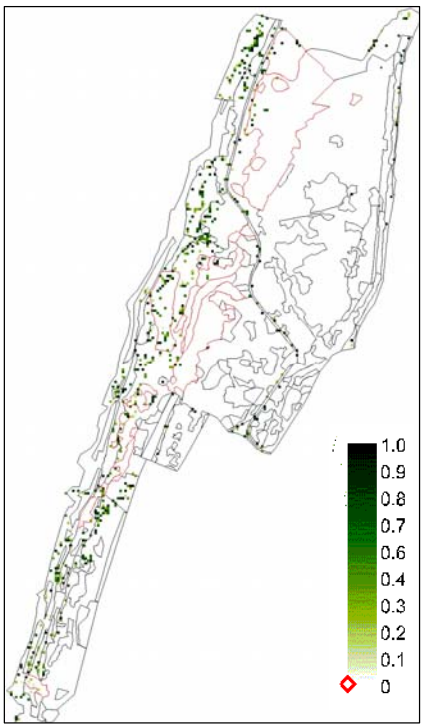

Figure 26: Spatial abundance map for Calamagrostis epigejos, derived from HyMap data. Millingerwaard, The Netherlands

Calamagrostis epigejos abundance map shows a middle correlation with the available vegetation map for the study area. The species is detected by remote sensing techniques for about half of the area where it is expected to appear. Additionally, certain pixels on the image are characterised with its reflectance spectra although in reality it is not present in the field. This fact may be due to confusion on the reflectance spectra with similar species, from the optical properties point of view.

According to the previous results pixels classified, as *Calamagrostis epigejos* in no expected areas would probably correspond to monocotyledonous specie with a low LAI value.

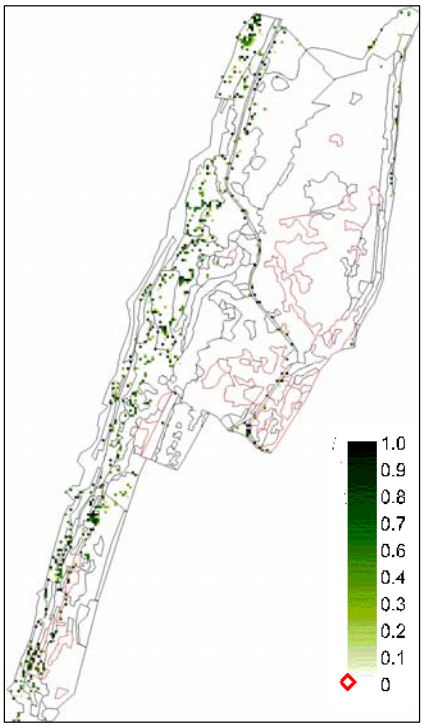

Figure 27: Spatial abundance map for Poa annua, derived from HyMap data. Millingerwaard, The Netherlands

Poa annua abundance is not predicted with consistent reliability. Only small areas where the species is expected are recognised for its spectral properties. However, it appears to be misunderstood with another species (the same ones that for the *Calamagrostis epigejos* case). This can be explained by the low LAI value, which causes low reflectance spectra at the canopy level.

The low reflectance values may be misunderstood by the soil reflectance values, considering its reflectance rate. Another possible explanation relies on the general ranges used to model this specie. No precise information was available, and it can have result in an underestimation of unique spectral properties.

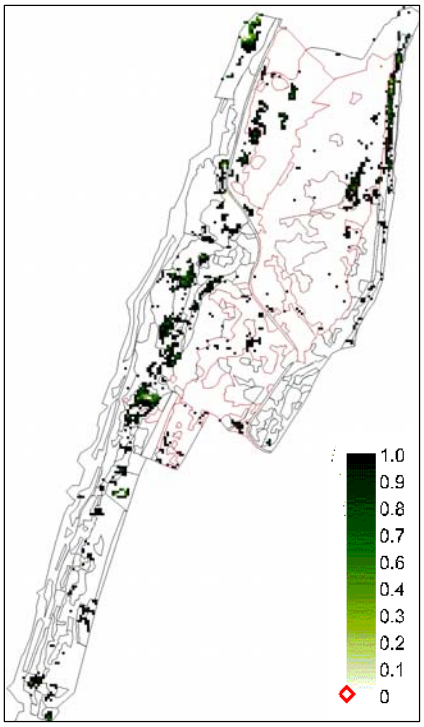

Figure 28: Spatial abundance map for Glechoma hederacea, derived from HyMap data. Millingerwaard, The Netherlands

Spectral recognition for *Glechoma hederacea* appears to be associated with high density areas of the specie. As can be appreciated in *figure 28*, the pixels classified for this specie appear to have a high abundance. However, most of them are slightly displaced from its expected location. This result can be due to different causes. One possibility is that the spatial coverage of the specie, as recorded from the sensor, is wider than its ground location.
On the other hand, from the spatial information for the measured relevees, this is one of the more extend species. Assuming that the relevee locations are representing the whole community area, the spectral properties for *Glechoma hederacea* could be misunderstood for another species with similar leaf structure and LAI value. In any case, the predicted locations for this species should be interpreted as mainly indicative.

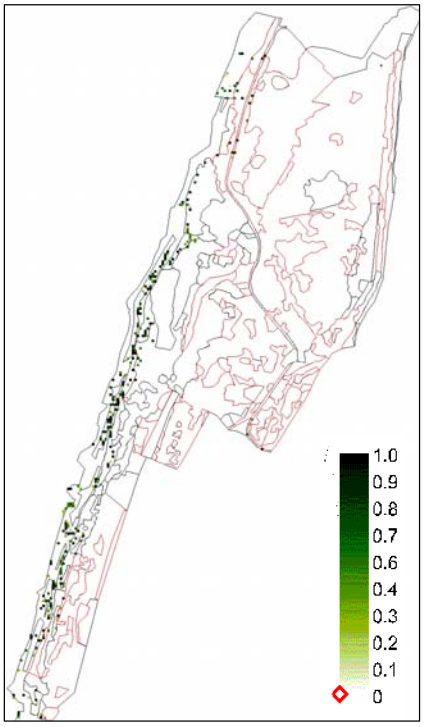

Figure 29: Spatial abundance map for Trifolium repens – Potentilla reptans, derived from HyMap data. Millingerwaard, The Netherlands

Trifolium repens in association with *Potentilla reptans* do not appear to be spectrally recognised from the sensor. The reason can be the weak characterisation for this species, due to the general ranges found in literature. Probably, biochemical and biophysical properties should be measured in the study area to be able to retrieve good abundance estimations.

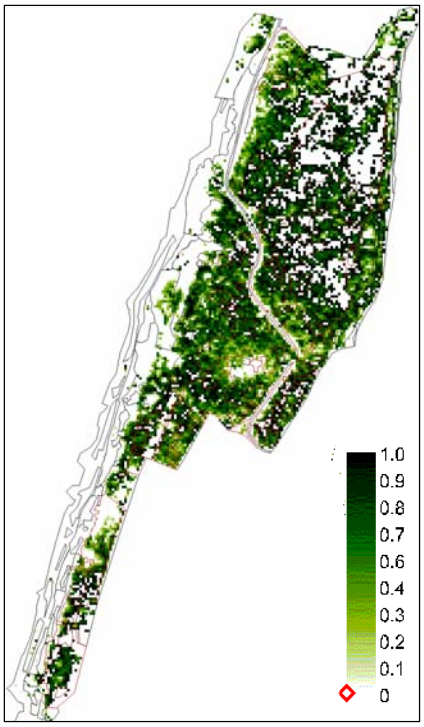

Figure 30: Spatial abundance map for Rubus caesius, derived from HyMap data. Millingerwaard, The Netherlands

Rubus caesius is the better-predicted case. Abundance estimations for this species appears in every area were it is expected to be in reality. Thus, it spectral properties have been very well retrieved and modelled. However, due to the large spatial coverage of the specie, mainly because their plants structure, it appears to mask other species that could be smaller. Additionally, the fact that it has the same average LAI value that for *Urtica dioica* could explain the results for that species, considering a misunderstood between its spectral properties.

As a conclusion, *Rubus caesius* is very well characterised by its biochemical and biophysical parameters, and its reflectance properties are very well modelled.

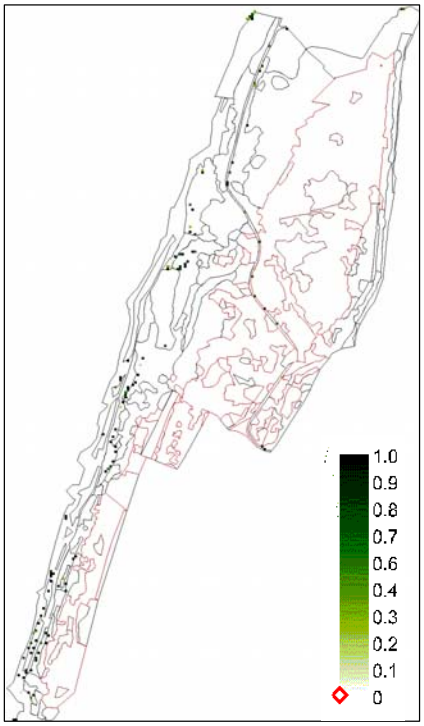

Figure 31: Spatial abundance map for Urtica dioica, derived from HyMap data. Millingerwaard, The Netherlands

Urtica dioica abundance is underestimated. Due to its high correlated spectral properties with *Glechoma hederacea, Trifolium repens and Rubus caesius*, its abundance is probably included in the correspondent maps instead that on the present one. Thus, the above mentioned species and *Urtica dioica* would be better estimated as a whole group than separately.

As a conclusion, *Urtica dioica* is underestimated by the applied procedure.

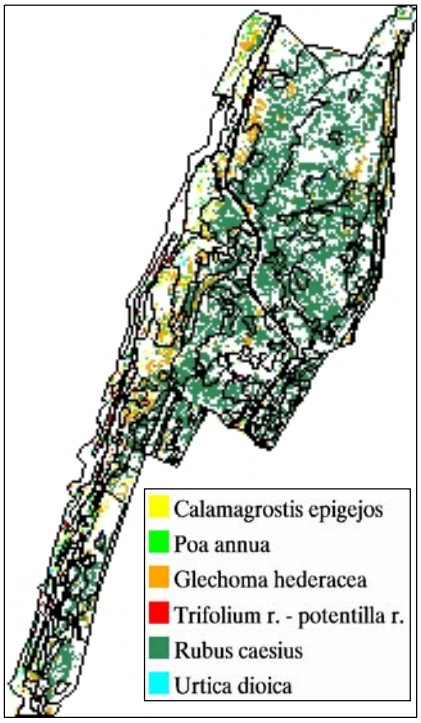

Figure 32: Abundance map for 6 species in the study area

Figure 32 shows the compilation of presented results for unconstrained linear spectral unmixing. Abundance values above 70% per species have been plotted together. When comparing this result whit the existing vegetation map of the area, differences can be appreciated. The main reason is that the existing map of the area classifies vegetation in community groups. Contrarily, this map represents the spatial abundance per single species. As settle down in the discussion of single abundance maps, some species abundances are poorly estimated. However, if we consider the main vegetation group, according to its spatial coverage, *Rubus caesius* is one of the dominant species. As can be appreciated in this figure, retrieved abundance for *Rubus caesius* is large, and it appears in the expected locations.

On the other hand, estimated abundance for grassland species (*Calamagrostis epigejos, Glechoma hederacea and Poa annua*) are underestimated when analysed independently. But if these abundances are grouped, we can observe that its location matches with vegetation communities corresponding to grassland species.
Thus, estimated abundances per species appear to be either under or over estimated, so should be interpreted with care, mainly for orientation purposes. Nevertheless, the potential of this result relies on considering species with similar biochemical and biophysical characteristics. Then, they can be used for predicting vegetation communities' location.

4.4.1.2- Fully Constrained Linear Spectral Unmixing

Fully Constrained Linear Spectral Unmixing was performed using the same endmembers as for the previous case (unconstrained case). The output resulted to widely differ from the ones obtained for the ULSU case. It is clear that the species whose spectral reflectance is higher mask the detection of species with lower reflectance values (especially monocotyledonous species and those with low LAI value). Then, these results cannot be considered as a good estimator of the abundances of species when using several species endmembers with different reflectance rates.

Furthermore, by applying this procedure, the assumption of fully representation of the study area by the used endmember is done. In reality, this is not true, as a larger number of species, soil types and other possible surfaces are present. So that, the inclusion of more endmembers would slightly in crease the quality of the results. However, due to the high biodiversity present in the area, no reliable estimations are expected.

Figures 33 to *38* correspond to obtained maps. In the cases where the map appears empty, no abundances are present because the procedure did not perform well for the present case. As opposite, in the cases where spatial abundance is shown, abundances are overestimated because the procedure did not perform well.

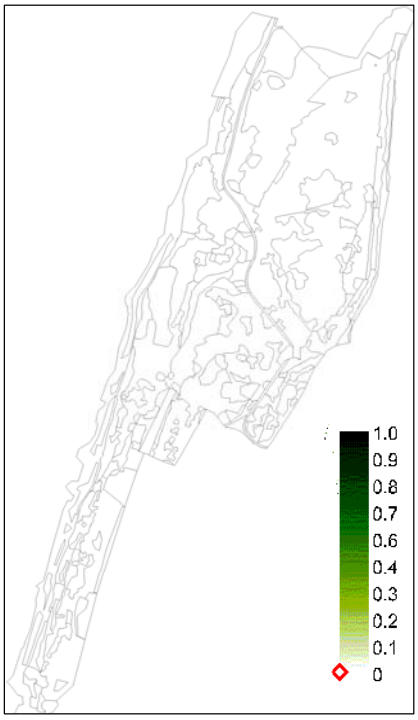

Figure 33: Spatial abundance map for Calamagrostis epigejos, derived from HyMap data. Millingerwaard, The Netherlands

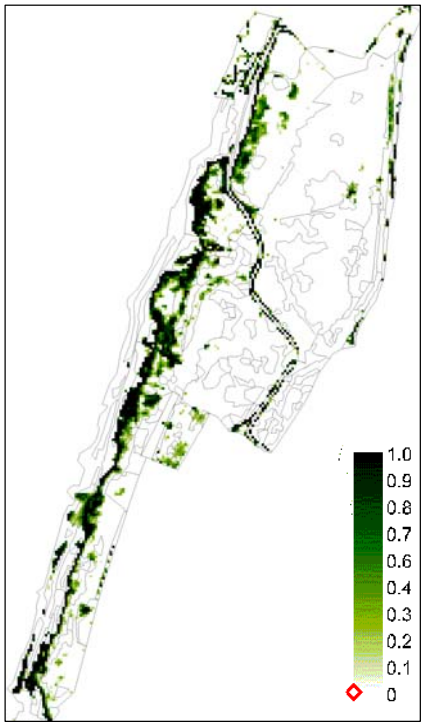

Figure 34: Spatial abundance map for Poa annua, derived from HyMap data. Millingerwaard, The Netherlands

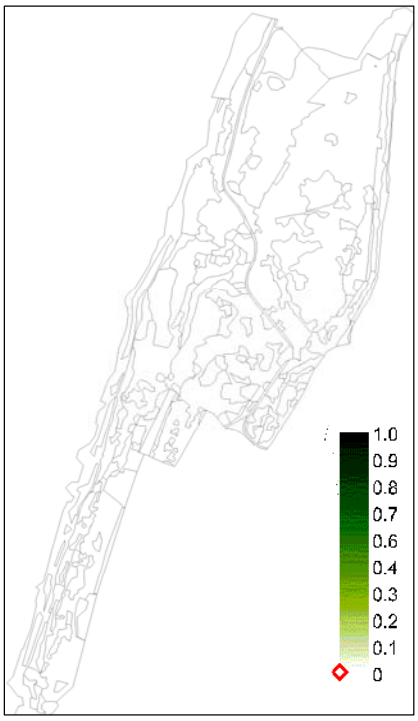

Figure 35: Spatial abundance map for Glechoma hederacea, derived from HyMap data. Millingerwaard, The Netherlands

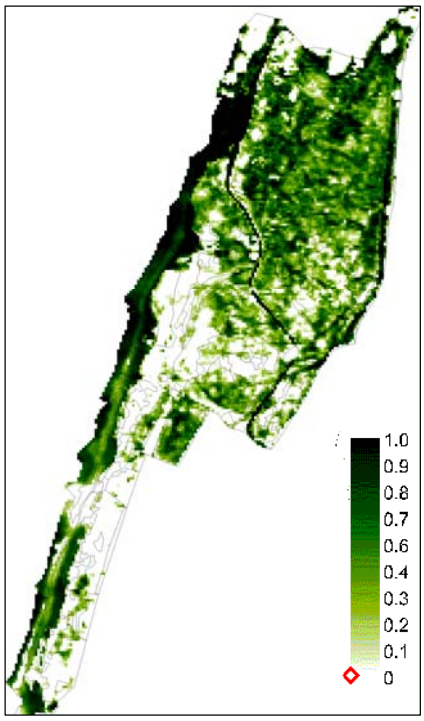

Figure 36: Spatial abundance map for Trifolium repens – Potentilla reptans, derived from HyMap data. Millingerwaard, The Netherlands

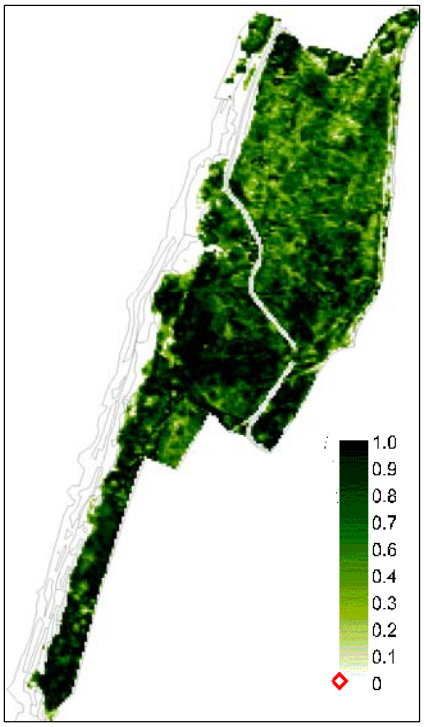

Figure 37: Spatial abundance map for Rubus caesius, derived from HyMap data. Millingerwaard, The Netherlands

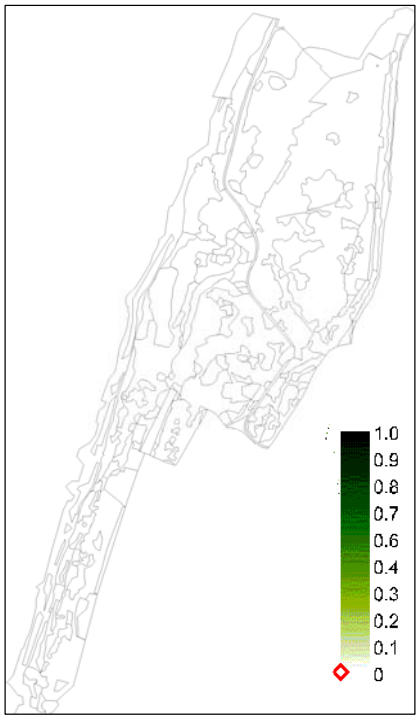

Figure 38: Spatial abundance map for Urtica dioica, derived from HyMap data. Millingerwaard, The Netherlands

4.4.2- Vegetation communities level

Unconstrained Linear Spectral Unmixing has been performed using vegetation communities, soil and water endmembers. The procedure has been applied to the best 6 simulated reflectance spectra. 3 different approaches can be applied: simulated signatures (*sim*), ground data (*can*) and image signatures (*im*).

When using simulated mixed spectra, abundances appear to be underestimated. This result is mainly obtained because water absorption features in the NIR part of the spectrum is smothered when mixing individual species spectra.
For the measured canopy reflectance spectra, results are also underestimated. The vegetation community is has been characterized by and average of 3 collected spectra. Then, it s expected than when using more ground data, results may improve. Additionally, if the vegetation community reflectance is not represented by only one spectrum, but with more (several endmembers correspond to the same vegetation community, and abundances can be compiled later), results are also expected to improve.

Considering the case when signatures from the image are used as endmembers result on an overestimation of the communities' abundances in relation with the previous approaches. The explanation may be that these signatures represent a HyMap image pixel (5 x 5 m.), while for the previous cases, a spectrometer measurement do not cover such a wide area.

Complete results are shown in *Appendix VII*. Further investigation has not been done as it lies out of the scope of the study. However, spatial statistic methods are recommended to investigate possible dependences and accuracy between and for each of the proposed approaches.

4.5- Quality assessment and ground validation

Table 10 show the correlations between modelled spectra per specie, for the study area. The similarity between certain species, considering its spectral properties, can explain the obtained results.

	Calamagrostis epigejos	***Glechoma hederacea***	***Trifollium repens***	***Poa annua***	***Rubus caesius***	***Urtica dioica***
Calamagrostis epigejos		0.976	0.976	0.999	0.983	0.980
Glechoma hederacea			0.998	0.981	0.991	0.999
Trifollium repens				0.984	0.996	0.999
Poa annua					0.991	0.986
Rubus caesius						0.995
Urtica dioica						

Table 10: Correlation between simulated reflectance spectra, per species.

As it can be derived from the table below, *Glechoma hederacea* and *Trifolium repens* abundances could be confused when performing the ULSU. In the same way, *Poa Annua* abundance would be misunderstood by *Calamagrostis epigejos* abundance.

The low abundance obtained for *Urtica dioica* can be justified by the high correlated spectra with *Glechoma hederacea* and *Trifolium repens*, that would be slightly overestimated. Thus, *Urtica dioica* abundance map appears to be underestimated, as it spectral properties would be masked by these two species.

Detailed graphs showing the correlations between species spectrum can be found in *Appendix VI*.

5- CONCLUSSIONS

Regarding the PROSPECT parameter retrieval, some conclusion can be drawn. It is clear the high influence of first guesses values. However, reliable results were obtained for the N and C_{ab} parameters. C_w and C_m are estimated in a weaker way. This may be due to the lower influence on the merit function of the model, used to simulate the reflectance spectra.

Spectral properties of different species can be related according to its biophysical properties. In this case, the concrete influence of LAI has been investigated. It is clear from the results that species show a higher correlation when having similar structural characteristics of the leaves (Monocotyledonous vs. Dicotyledonous). Considering the LAI parameter, species with similar value have a higher correlated spectral properties that those ones with very different LAI values. This conclusion was esxpected, due to the determining influence on the surface properties (the leaf surface, in this case) on the reflectance spectra, and the construction of SAIL model (Verhoef, 1984).

Unconstrained Linear Spectral Unmixing show good results to disthinguis species according to their structural properties. 6 species appeared to be the optimum number regarding the accuracy of the abundance estimations. However, this results must be interpreted with care, as some species appear to be mistaken, due to their high correlated spectral properties.

Contrarily, Fully Constrained Linear Unmixing does not give good results. This fact can be due to the indirect assumption that all the vegetation is represented by the used endmembers. Additionally, it can be noticed that those species with higher reflectance values (in concrete, in the NIR part of the spectrum), mask the appearance of species with lower reflectance rates (monocotyledonous and low LAI species). Thus, this technique is not worthy for the present study.

At the vegetation community level, Unconstrained Linear Spectral Unmixing can be applied following different approaches. As an “a priori” conclusion, it is clear that the use of endmembers directly derived from the image reflectance overestimates the abundances of vegetation communities. Additionally, simulated spectra from the SAIL model seem to underestimate the endmember abundances. The same conclusion can be applied to Canopy reflectance measurements. However, a spatial statistic analysis is recommended in order to investigate the accuracy of the result. This analysis was not performed as it lies out of the scope of the present study.

6- RECOMMENDATIONS

6.1- Scope of the study

From the fieldwork, transmittance data at the leaf level for the measured species is available. In case of including it on the PROSPECT inversion, biochemical parameters estimation would improve its accuracy (Fourty *et al*.,1996). Additionally, chlorophyll, water, and dry matter content can be estimated from the inversion of PROSPECT model (Jacquemoud *et al*., 1996). However, the accuracy of the estimations could be improved by fitting the simulated spectra to specific ranges of the measured reflectance spectra.

In case of applying the same methodology described in this study, it is recommended to narrow the simulated LAI intervals within the SAIL model. In this case, a more accurate characterization of the spectral properties of pure species would be expected.

Regarding the Linear Spectral Unmixing, the unconstrained case is the most reliable technique for the retrieval of abundance maps in the study area. These results can be extrapolated to areas with a high vegetation biodiversity, where not all the possible vegetation species (endmembers) can be characterised. Thus, Fully Constrained Spectral Unmixing should only be use in the case where all the possible endmembers can be assumed to be known.

6.2- Future research

Chlorophyll content can be estimated from PROSPECT model inversion. To do so, it is recommended to use only the 400 – 700 nm range of the reflectance spectra. Additionally, the obtained results could be linked to the available data for the study area regarding the nitrogen content, as this element is present in the chlorophyll molecule (Johnson, 2001; Le Maire *et al*., 2003).
In the same line, dry matter content could be compared with the dry matter measured by the Ecology group. Water absorption bands have been removed from the dataset for this study. However, when keeping those bands, research could be done on the influence of water content on the reflectance spectra at the foliage and canopy level (Carter, 1991; Ceccato *et al*., 2001; Sims, 2002; Zarco-Tejada *et al*., 2003).

The presented approach can be applied to the forest area of the Millingerwaard. In the future, validated biophysical parameters values for this area will be available. Thus, spectral libraries presented for the PROSPECT model can be used as an input for the SAIL model, and accurate simulation at the canopy level could be done.

Starting from the obtained results for the Unconstrained Linear Spectral Unmixing performance, it is recommended to continue with the same methodology. However, more data is needed in order to characterize more vegetation species. The Fully Constrained Linear Spectral Unmixing is not recommended for use, due to the high biodiversity of the study area.
At the Community level case, further research has to be done, in order to investigate its reliability. In order to do so, and spatial statistical approach is recommended.

7- ACKNOWLEDGMENTS

I am grateful to all the people that, in many ways, contributed to this study.
First of all, I would like to express my gratitude to my supervisors, Michael Schaepman and Lammert Kooistra, that always helped and guided me, suggesting ideas, solving my doubts and motivating me on my research.
I would also like to thank Raul Zurita, for all his help, ideas, interest, and patience with the steps performed in Matlab.
There are also a lot of people that helped me during all my thesis period. Sitze de Bruin, Anne Schmidt, and Han van Dooben contributed to make from the fieldwork a nice experience. Karle Sykora asisted me on the ecological side of this study. Gabriela Schaepman provided and assisted me with the models, and Allard de Wit helped me when having programming problems.

Of course I can not forget all my mates in Alterra, that made the working days nice, finding always a moment for a laugh: Angela, Jie, Taye, Worku, Babs, Lucy, Teshome, Jochem, Lucia, Tine and Arjan.

Special thanks to my family, that supported and encouraged me at all the moments of my stay in The Netherlands.
My friends always had a smile for me, in any possible way, in person or by mail and internet when they were far away.
Roland and Jordis supported me despite the distance; Sara, Uxue, and Maria made me belive in myself; Eneko, Sonia, and Beatriz are always a reason to visit my home town. Celia, Patricia, Marga and Andres always had a cup of coffe for me and Jonah, Veronique, and Anna made my life in The Netherlands something more than a study year.

Last but not least, I want to thank my brother, Pablo, for always finding a moment for 2 hours of conversation.

8- REFERENCES

Almeida, T.I.R., De Souza Filho, C.R., 2004. Principal component analysis applied to feature-oriented band ratios of hyperspectral data: A tool for vegetation studies. International Journal of Remote Sensing 25, 5005-5023.

Anten, N.P.R., Hirose, T., Anten, N.P.R., 1999. Interspecific differences in above-ground growth patterns result in spatial and temporal partitioning of light among species in a tall-grass meadow. Journal of Ecology 87, 583-597.

Baret, F., Clevers, J.G., Steven, M.D., 1995. The robustness of canopy gap fraction estimates from red and near-infrared reflectances: A comparison of approaches. Remote Sensing of Environment 54, 141-151.

Borel, C.C., Gerstl, S.A.W., 1994. Nonlinear spectral mixing models for vegetative and soil surfaces. Remote Sensing of Environment 47, 403-416.

Calvao, T., Palmeirim, J.M., 2004. Mapping Mediterranean scrub with satellite imagery: Biomass estimation and spectral behaviour. International Journal of Remote Sensing 25, 3113-3126.

Clevers, J.G.P.W., 1986. The derivation of a simplified reflectance model for the estimation of LAI. Remote sensing for resources development and environmental management. Proc. 7th ISPRS Commission VII symposium, Enschede, 1986. Vol. 1, 215-220.

Clevers, J.G.P.W., 1988. The derivation of a simplified reflectance model for the estimation of leaf area index. Remote Sensing of Environment 25, 53-69.

Coops, N.C., Culvenor, D.S., Stone, C., Chisholm, L.A., Merton, R.N., 2003. Chlorophyll content in eucalypt vegetation at the leaf and canopy scales as derived from high resolution spectral data. Tree Physiology 23, 23-31.

Curran, P.J., 1989. Remote sensing of foliar chemistry. Remote Sensing of Environment 30, 271-278.

Curran, P.J., Dungan, J.L., Peterson, D.L., 2001. Estimating the foliar biochemical concentration of leaves with reflectance spectrometry: Testing the Kokaly and Clark methodologies. Remote Sensing of Environment 76, 349-359.

Fourty, T., Baret, F., Fourty, T., Jacquemoud, S., Schmuck, G., Verdebout, J., 1996. Leaf optical properties with explicit description of its biochemical composition: Direct and inverse problems. Remote Sensing of Environment 56, 104-117.

Fourty, T., Baret, F., Jacquemoud, S., Schmuck, G., Verdebout, J., 1996. Leaf optical properties with explicit description of its biochemical composition: Direct and inverse problems. Remote Sensing of Environment 56, 104-117.

Fourty, T.H., Baret, F., 1998. On spectral estimates of fresh leaf biochemistry. International Journal of Remote Sensing 19, 1283-1297.

Fuentes, D.A., Gamon, J.A., Qui, H.-L., Sims, D.A., Roberts, D.A., 2001. Mapping Canadian boreal forest vegetation using pigment and water absorption features derived from the AVIRIS sensor. Journal of Geophysical Research D: Atmospheres 106, 33565-33577.

Garcia-Haro, F.J., Gilabert, M.A., Melia, J., 1999. Extraction of Endmembers from Spectral Mixtures. Remote Sensing of Environment 68, 237-253.

García-Haro, F.J., Gilabert, M.A., Meliá, J., 1996. Linear spectral mixture modelling to estimate vegetation amount from optical spectral data. International Journal of Remote Sensing 17, 3373-3400.

Isabel Geloof, I., de Ronde, I., 2002. De vegetatie van de Millingerwaard na 10 jaar natuurbeheer. Centre for Geo - Information Wageningen, Wageningen University.

Gilabert, M.A., Garcia-Haro, F.J., Melia, J., 2000. A Mixture Modeling Approach to Estimate Vegetation Parameters for Heterogeneous Canopies in Remote Sensing. Remote Sensing of Environment 72, 328-345.

Gillon, D., Hernando, C., Valette, J.-C., Joffre, R., 1997. Fast estimation of the calorific values of forest fuels by near-infrared reflectance spectroscopy. Canadian Journal of Forest Research 27, 760-765.

Gillon, D., Joffre, R., Ibrahima, A., 1999. Can litter decomposability be predicted by near infrared reflectance spectroscopy? Ecology 80, 175-186.

Govaerts, Y.M., Verstraete, M.M., Jacquemoud, S., Ustin, S.L., 1996. Three-dimensional radiation transfer modeling in a dicotyledon leaf. Applied Optics 35, 6585-6598.

Grossman, Y.L., Ustin, S.L., Jacquemoud, S., Sanderson, E.W., Schmuck, G., Verdebout, J., 1996. Critique of stepwise multiple linear regression for the extraction of leaf biochemistry information from leaf reflectance data. Remote Sensing of Environment 56, 182-193.

Heinz, D.C., Chang, C.-I., 2001. Fully constrained least squares linear spectral mixture analysis method for material quantification in hyperspectral imagery. IEEE Transactions on Geoscience and Remote Sensing 39, 529-545.

Ingram, J.C., Dawson, T.P., Whittaker, R.J., Ingram, J.C., 2005. Mapping tropical forest structure in southeastern Madagascar using remote sensing and artificial neural networks. Remote Sensing of Environment 94, 491-507.

Jacquemoud, S., Baret, F., 1990. PROSPECT: A model of leaf optical properties spectra. Remote Sensing of Environment 34, 75-91.

Jacquemoud, S., Ustin, S.L., Verdebout, J., Schmuck, G., Andreoli, G., Hosgood, B., 1996. Estimating leaf biochemistry using the PROSPECT leaf optical properties model. Remote Sensing of Environment 56, 194-202.

Jago, R.A., Cutler, M.E.J., Curran, P.J., Jago, R.A., 1999. Estimating canopy chlorophyll concentration from field and airborne spectra. Remote Sensing of Environment 68, 217-224.

Johnson, L.F., 2001. Nitrogen influence on fresh-leaf NIR spectra. Remote Sensing of Environment 78, 314-320.

Kooistra, L., Sterkx, S., Liras Laita, E., Mengesha, T., Verbeiren, B., Battellaan, O., van Dobben, H., Schaepman, M., 2005. HyEco04: an airborne imaging spectroscopy campaign in the floodplain Millingerwaard, Alterra-report.

Le Maire, G., François, C., Dufrêne, E., 2004. Towards universal broad leaf chlorophyll indices using PROSPECT simulated database and hyperspectral reflectance measurements. Remote Sensing of Environment 89, 1-28.

McMorrow, J.M., Evans, M.G., Al-Roichdi, A., Cutler, M.E.J., 2004. Hyperspectral indices for characterizing upland peat composition. International Journal of Remote Sensing 25, 313-325.

Mengesha, T. 2005. Validation of ground biophysical products using Imaging Spectroscopy in softwood forest. Centre for Goeinformation Wageningen, Wageningen University.

Müllerova, J., 2005. Use of digital aerial photography for sub-alpine vegetation mapping: A case study from the Krkonose Mts., Czech Republic. Plant Ecology 175, 259-272.

Rahman, A.F., Gamon, J.A., Sims, D.A., Schmidts, M., Rahman, A.F., 2003. Optimum pixel size for hyperspectral studies of ecosystem function in southern California chaparral and grassland. Remote Sensing of Environment 84, 192-207.

Schaepman, M.E., Koetz, B., Schaepman-Strub, G., Itten, K.I., 2005. Spectrodirectional remote sensing for the improved estimation of biophysical and -chemical variables: Two case studies. International Journal of Applied Earth Observation and Geoinformation 6, 271-282.

Schaepman, M., D. Schläpfer, and A. Müller, 2001. Performance Requirements for Airborne Imaging Spectrometers, Proc. SPIE, Imaging Spectrometry VII, Vol. 4480, 23–31,

Schaminée, J.H.J., van Kley, J.E., Ozinga, W.A., 2002. The analysis of long-term changes in plant communities: Case studies from the Netherlands. Phytocoenologia 32, 317-335.

Settle, J., Campbell, N., 1998. On the errors of two estimators of sub-pixel fractional cover when mixing is linear. IEEE Transactions on Geoscience and Remote Sensing 36, 163-170.

Settle, J.J., Drake, N.A., 1993. Linear mixing and the estimation of ground cover proportions. International Journal of Remote Sensing 14, 1159-1177.

Sims, D.A., Gamon, J.A., 2002. Relationships between leaf pigment content and spectral reflectance across a wide range of species, leaf structures and developmental stages. Remote Sensing of Environment 81, 337-354.

Sims, D.A., Gamon, J.A., 2003. Estimation of vegetation water content and photosynthetic tissue area from spectral reflectance: A comparison of indices based on liquid water and chlorophyll absorption features. Remote Sensing of Environment 84, 526-537.

T.H., F., F., B., 1998. On spectral estimates of fresh leaf biochemistry. International Journal of Remote Sensing, 1283-1297.

Thomas, V., Treitz, P., Jelinski, D., McCaughey, J.H., Miller, J., Lafleur, P., 2003. Image classification of a northern peatland complex using spectral and plant community data. Remote Sensing of Environment 84, 83-99.

Underwood, E., Ustin, S., DiPietro, D., 2003. Mapping nonnative plants using hyperspectral imagery. Remote Sensing of Environment 86, 150-161.

Ustin, S.L., Roberts, D.A., Gardner, M., Dennison, P., 2002. Evaluation of the potential of hyperion data to estimate wildfire hazard in the Santa Ynez Front Range, Santa Barbara, California. International Geoscience and Remote Sensing Symposium (IGARSS) 2, 796-798.

Verbrugghe, M., Cierniewski, J., 1995. Effects of sun and view geometries on cotton bidirectional reflectance. Test of a geometrical model. Remote Sensing of Environment 54, 189-197.

Verhoef, W., 1984. Light scattering by leaf layers with application to canopy reflectance modeling: the SAIL model. Remote Sensing of Environment 16, 125-141.

Verhoef, W., Bach, H., 2003. Simulation of hyperspectral and directional radiance images using coupled biophysical and atmospheric radiative transfer models. Remote Sensing of Environment 87, 23-41.

Verhoef, W., Bach, H., 2003. Remote sensing data assimilation using coupled radiative transfer models. Physics and Chemistry of the Earth 28, 3-13.

Weiser, R.L., Asrar, G., Miller, G.P., Kanemasu, E.T., 1986. Assessing grassland biophysical characteristics from spectral measurements. Remote Sensing of Environment 20, 141-152.

Zhang, Q., Chen, W., Latifovic, R., Fraser, R., Cihlar, J., Zhang, Q., Pavlic, G., 2004. Deriving stand age distribution in boreal forests using SPOT VEGETATION and NOAA AVHRR imagery. Remote Sensing of Environment 91, 405-418.

Online references:

Integrated spectronics: http://www.intspec.com

Website on leaf optical properties website on leaf optical properties (Database by Dr. Stéphane Jacquemoud): http://membres.lycos.fr/opticleaf

Radiative transfer model intercomparison:
http://rami-benchmark.jrc.it/HTML/Home.php

RSI website: http://www.rsinc.com

Biodiversity data portal: http://www.gbif.net/portal/index.jsp

Expertise database for invasive species: http://www.invasivespecies.gov

PLANTS Database (Unites States department of Agriculture): http://plants.usda.gov

APPENDICES

APPENDIX I:
HYMAP™ AIRBORNE IMAGING SENSOR

The HyMap sensor is an airborne imaging system that is used for earth resources remote sensing. It records a digital image of the earth's sunlit surface underneath the aircraft but unlike standard aerial cameras, the HyMap records images in a large number of wavelengths. In essence, the HyMap is an airborne spectrometer and like spectrometers used in analytical chemistry, it can detect and identify materials by the spectral features contained in the recorded data.

The HyMap records an image of the earth's surface by using a rotating scan mirror which allows the image to build line by line as the aircraft flies forward. The reflected sunlight collected by the scan mirror is then dispersed into different wavelengths by four spectrometers in the system. The spectral and image information from the spectrometers is digitised and recorded on tape.

To minimise distortion induced in the image by aircraft pitch, roll and yaw motions, the HyMap is mounted in a gyro-stabilised platform. While the platform minimises the effects of aircraft motion, small image distortions remain. These residual motions are monitored with a 3 axis gyro, 3 axis accelerometer system (IMU – Inertial Measurement Unit). The system currently used with the HyMap is a Boeing C-MIGITS II.

Associated with the actual HyMap optical system is an electronics sub-system which is rack mounted in the aircraft. This electronics sub-system provides the sensor with power and contains a computer system that controls the data acquisition process. There is a touch screen monitor used by the operator to set data acquisition parameters, start and stop recording, view the image as it is being acquired and review various engineering status indicators (power, temperature etc).

The HyMap system has been designed to operate in aircraft that have standard aerial photo-ports. The angular width of the recorded image is 61.3 degrees or about 2.3 km when operating 2000m above ground level. Typically, the spatial resolution achieved with the HyMap is in the range 3 to 10 m.
The general technical specifications of the HyMap system are given in the tables below:

Spatial Configurations	
IFOV	2.5 mr along track 2.0 mr across track
FOV	61.3 degrees (512 pixels)
Swath	2.3 km at 5m IFOV (along track) 4.6 km at 10m IFOV (along track)

Table I: HyMap Spatial Parameters

Typical Spectral Configuration			
Module	**Spectral range**	**Bandwidth across module**	**FWHM**
VIS	0.45 – 0.89 μm	15 – 16 nm	15 nm
NIR	0.89 – 1.35 μm	15 – 16 nm	15 nm
SWIR1	1.40 – 1.80 μm	15 – 16 nm	13 nm
SWIR2	1.95 – 2.48 μm	18 – 20 nm	17 nm

Table II: Spectral band positions of HyMap (Cocks et al, 1998)

The following figure shows the HyMap mounted on a Do 228.

FigureI: HyMap in its stabilised platform mounted in a DLR Do 228

I.I- Hyperspectral images (HyMap) for Linear Spectral Unmixing

The HyMap sensor is a 128 channel high resolution imaging spectrometer. It operates within the wavelength range from 450 to 2480 nm.
It has a signal to noise ratio up to 500:1. Signal to noise ratio is one of the most important indicators of data quality considering hyperspectral data. To calculate it, the following formula can be applied (Schowengerdt, 1997):

$SNR_i = DN_i / \sigma_i$

With: SNR_i = signal to noise ratio in channel *i*
DN_i = Mean in channel *i*
σ_i = Standard Deviation in channel *i*

HyMap images can be processed in order to asses Linear Spectral Unmixing. This approach consists on modelling the spectral reflectance signature as a mixture of pure features named endmembers. Linear Spectral Unmixing analysis assumes that most of the spectral variations in multispectral images are due to a mixture of the different reflectance spectra of a limited number of surface materials (i.e. vegetation and soil). These different reflectance spectra mix at the sub pixel scale, producing mixed pixel spectra.
As first approach, spectral unmixing can be considered a linear combination of pure components (endmembers) spectra (Hill, 1993).

$R_\lambda = \Sigma^{n}_{i=1} f_i \times r_{i\lambda} + \varepsilon_i$

where R_λ is the reflectance of mixed pixel in wavelength λ, f_i is the abundance of the endmember *i*, $r_{i\lambda}$ is the reflectance of the component I in wavelength λ and ε_I is the residual error in wavelength λ.

I.II- Data Processing Information

Name of Project			HyEco			
Date of Acquisition			28.07.2004 & 02.08.2004			
Resampling Method (orthorectification)			Bilinear			
Map projection			UTM, Zone 31N			
Geodetic datum			WGS-84			
Strip Number	**Flight Altitude**	**Scan Frequency**	**Flight Heading**	**Solar Azimuth**	**Solar Zenith**	**Pixel Size**
1	2300 m (asl)	16 Hz	0°			5x5 m
2	2300 m (asl)	16 Hz	180°			
1	2380 m (asl)	16 Hz	0°			5x5 m
2	2380 m (asl)	16 Hz	180°			5x5 m
3	2380 m (asl)	16 Hz	330°			5x5 m

Table IIIXI: Data Processing Information of the specific Project

I.III- HyMap Quick looks

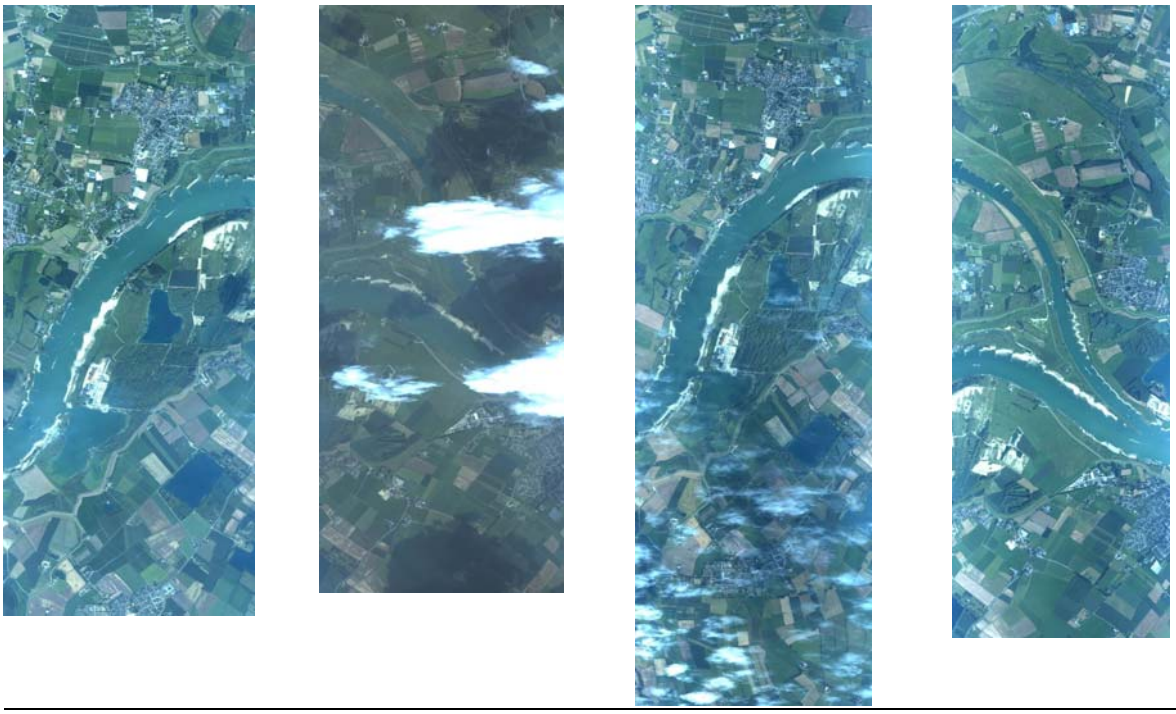

Figure II: HyMap Quick looks

APPENDIX II:
PLANT PROFILE AND TAXONOMICAL CLASSIFICATION

Specie_code	Specie	Group	Growth Habit	Duration
Achilmil	*Achillea millefolium*	Dicot	Forb/herb	Perennial
Agrossto	*Agrostis stolonifera*	Monocot	Graminoid	Perennial
Arctilap	*Arctium lappa*	Dicot	Forb/herb	Biennial
Arrheela	*Arrhenatherum elatius*	Monocot	Graminoid	Perennial
Atrippat	*Atriplex patula*	Dicot	Forb/herb	Annual
Brassnig	*Brassica nigra*	Dicot	Forb/herb	Annual
Bromuine	*Bromus inermis*	Monocot	Graminoid	Perennial
Calamepi	*Calamagrostis epigejos*	Monocot	Graminoid	Perennial
Calyssep	*Calystegia sepium*	Dicot	Forb/herb	Perennial
Cardunut	*Carduus nutans*	Dicot	Forb/herb	Biennial/Perennial
Carexhir	*Carex hirta*	Monocot	Graminoid	Perennial
Cerasfon	*Cerastium fontanum*	Dicot	Forb/herb	Biennial/Perennial
Cirsiarv	*Cirsium arvense*	Dicot	Forb/herb	Perennial
Cirsivul	*Cirsium vulgare*	Dicot	Forb/herb	Biennial
Cratamon	*Crataegus monogyna*	Dicot	Shrub	Perennial
Cynoddac	*Cynodon dactylon*	Monocot	Graminoid	Perennial
Dactyglo	*Dactylis glomerata*	Monocot	Graminoid	Perennial
Dipsaful	*Dipsacus fullonum*	Dicot	Forb/herb	Biennial
Elymurep	*Elymus repens*	Monocot	Graminoid	Perennial
Epilohir	*Epilobium hirsutum*	Dicot	Forb/herb	Perennial
Epilotet	*Epilobium tetragonum*	Dicot	Forb/herb	Perennial
Equisarv	*Equisetum arvense*	Horsetail	Forb/herb	Perennial
Erigecan	*Erigeron canadensis*	Dicot	Forb/herb	Annual/Biennial
Eryngcam	*Eryngium campestre*	Dicot	Forb/herb	Perennial
Euphocyp	*Euphorbia cyparissias*	Dicot	Forb/herb	Perennial
Euphoesu	*Euphorbia esula*	Dicot	Forb/herb	Perennial
Festurub	*Festuca rubra*	Monocot	Graminoid	Perennial
Galeotet	*Galeopsis tetrahit*	Dicot	Forb/herb	Annual
Galiuapa	*Galium aparine*	Dicot	Forb/herb	Perennial
Galiumol	*Galium mollugo*	Dicot	Forb/herb	Perennial
Geranpus	*Geranium pusillum*	Dicot	Forb/herb	Annual/Biennial
Glechhed	*Glechoma hederacea*	Dicot	Forb/herb	Perennial
Hernigla	*Herniaria glabra*	Dicot	Forb/herb	Annual/Perennial
Hyperper	*Hypericum perforatum*	Dicot	Forb/herb	Perennial
Iris pse	*Iris pseudacorus*	Monocot	Forb/herb	Perennial
Linarvul	*Linaria vulgaris*	Dicot	Forb/herb	Perennial
Loliuper	*Lolium perenne*	Monocot	Graminoid	Annual/Biennial/Perennial
Lycopeur	*Lycopus europaeus*	Dicot	Forb/herb	Perennial
Lythrsal	*Lythrum salicaria*	Dicot	Forb/herb	Perennial
Matrimar	*Matricaria maritima*	Monocot	Graminoid	Annual/Biennial/Perennial
Mediclup	*Medicago lupulina*	Dicot	Forb/herb	Annual/Perennial
Melilalt	*Melilotus altissima*	Dicot	Forb/herb	Biennial/Perennial
Menthaqu	*Mentha aquatica*	Dicot	Forb/herb	Perennial
Myosoarv	*Myosotis arvensis*	Dicot	Forb/herb	Annual
Myosol-c	*Myosotis laxa (subsp. cespitosa)*	Dicot	Forb/herb	Annual/Biennial/Perennial
Odontver	*Odontites vernus*	Dicot	Forb/herb	Annual

Odontv-s	*Odontites vernus subsp. serotinus*	Dicot	Forb/herb	Annual
Oenotbie	*Oenothera biennis*	Dicot	Forb/herb	Biennial
Pastisat	*Pastinaca sativa*	Dicot	Forb/herb	Biennial/Perennial
Phalaaru	*Phalaris arundinacea*	Monocot	Graminoid	Perennial
Phleupra	*Phleum pratense*	Monocot	Graminoid	Perennial
Plantlan	*Plantago lanceolata*	Dicot	Forb/herb	Annual/Biennial/Perennial
Plantmaj	*Plantago major*	Dicot	Forb/herb	Perennial
Poa ann	*Poa annua*	Monocot	Graminoid	Annual/Biennial
Poa pra	*Poa pratensis*	Monocot	Graminoid	Perennial
Poa tri	*Poa trivialis*	Monocot	Graminoid	Perennial
Polynper	*Polygonum persicaria*	Dicot	Forb/herb	Annual/Perennial
Potenans	*Potentilla anserina*	Dicot	Forb/herb	Perennial
Potenrep	*Potentilla reptans*	Dicot	Forb/herb	Perennial
Prunevul	*Prunella vulgaris*	Dicot	Forb/herb	Perennial
Ranunrep	*Ranunculus repens*	Dicot	Forb/herb	Perennial
Roripaus	*Rorippa austriaca*	Dicot	Forb/herb	Perennial
Rubuscae	*Rubus caesius*	Dicot	Shrub	Perennial
Rumexace	*Rumex acetosa*	Dicot	Forb/herb	Perennial
Rumexcri	*Rumex crispus*	Dicot	Forb/herb	Perennial
Rumexobt	*Rumex obtusifolius*	Dicot	Forb/herb	Perennial
Saponoff	*Saponaria officinalis*	Dicot	Forb/herb	Perennial
Seneceru	*Senecio erucifolius*	Dicot	Forb/herb	Perennial
Senecina	*Senecio inaequidens*	Dicot	Forb/herb	Perennial
Senecjac	*Senecio jacobaea*	Dicot	Forb/herb	Perennial
Solandul	*Solanum dulcamara*	Dicot	Forb/herb	Perennial
Solidcan	*Solidago canadensis*	Dicot	Forb/herb	Perennial
Stellaqu	*Stellaria aquatica*	Dicot	Forb/herb	Perennial
Tanacvul	*Tanacetum vulgare*	Dicot	Forb/herb	Perennial
Taraxoff	*Taraxacum officinale s.s.*	Dicot	Forb/herb	Perennial
Trifofra	*Trifolium fragiferum*	Dicot	Forb/herb	Perennial
Triforep	*Trifolium repens*	Dicot	Forb/herb	Perennial
Urticdio	*Urtica dioica*	Dicot	Forb/herb	Perennial
Verbanig	*Verbascum nigrum*	Dicot	Forb/herb	Perennial

TableIV: Plant profile for the vegetation species in the Millingerwaard

Specie_code	Specie	Kingdom	Division	Class	Order	Family	Genus
Achilmil	*Achillea millefolium*	Plantae	Magnoliophyta	Magnoliopsida	Asterales	Asteraceae	Achillea
Agrossto	*Agrostis stolonifera*	Plantae	Magnoliophyta	Liliopsida	Cyperales	Poaceae	Agrostis
Arctilap	*Arctium lappa*	Plantae	Magnoliophyta	Magnoliopsida	Asterales	Asteraceae	Arctium
Arrheela	*Arrhenatherum elatius*	Plantae	Magnoliophyta	Liliopsida	Cyperales	Poaceae	Arrhenatherum
Atrippat	*Atriplex patula*	Plantae	Magnoliophyta	Magnoliopsida	Caryophyllales	Chenopodiaceae	Atriplex
Brassnig	*Brassica nigra*	Plantae	Magnoliophyta	Magnoliopsida	Capparales	Brassicaceae	Brassica
Bromuine	*Bromus inermis*	Plantae	Magnoliophyta	Liliopsida	Cyperales	Poaceae	Bromus
Calamepi	*Calamagrostis epigejos*	Plantae	Magnoliophyta	Liliopsida	Cyperales	Poaceae	Calamagrostis
Calyssep	*Calystegia sepium*	Plantae	Magnoliophyta	Magnoliopsida	Solanales	Convolvulaceae	Calystegia
Cardunut	*Carduus nutans*	Plantae	Magnoliophyta	Magnoliopsida	Asterales	Asteraceae	Carduus
Carexhir	*Carex hirta*	Plantae	Magnoliophyta	Liliopsida	Cyperales	Cyperaceae	Carex
Cerasfon	*Cerastium fontanum*	Plantae	Magnoliophyta	Magnoliopsida	Caryophyllales	Caryophyllaceae	Cerastium
Cirsiarv	*Cirsium arvense*	Plantae	Magnoliophyta	Magnoliopsida	Asterales	Asteraceae	Cirsium
Cirsivul	*Cirsium vulgare*	Plantae	Magnoliophyta	Magnoliopsida	Asterales	Asteraceae	Cirsium
Cratamon	*Crataegus monogyna*	Plantae	Magnoliophyta	Magnoliopsida	Rosales	Rosaceae	Crataegus L.
Cynoddac	*Cynodon dactylon*	Plantae	Magnoliophyta	Liliopsida	Cyperales	Poaceae	Cynodon
Dactyglo	*Dactylis glomerata*	Plantae	Magnoliophyta	Liliopsida	Cyperales	Poaceae	Dactylis
Dipsaful	*Dipsacus fullonum*	Plantae	Magnoliophyta	Magnoliopsida	Dipsacales	Dipsacaceae	Dipsacus
Elymurep	*Elymus repens*	Plantae	Magnoliophyta	Liliopsida	Cyperales	Poaceae	Elymus
Epilohir	*Epilobium hirsutum*	Plantae	Magnoliophyta	Magnoliopsida	Myrtales	Onagraceae	Epilobium
Epilotet	*Epilobium tetragonum*	Plantae	Magnoliophyta	Magnoliopsida	Myrtales	Onagraceae	Epilobium
Equisarv	*Equisetum arvense*	Plantae	Equisetophyta	Equisetopsida	Equisetales	Equisetaceae	Equisetum
Erigecan	*Erigeron canadensis*	Plantae	Magnoliophyta	Magnoliopsida	Asterales	Asteraceae	Conyza Less.
Eryngcam	*Eryngium campestre*	Plantae	Magnoliophyta	Magnoliopsida	Apiales	Apiaceae	Eryngium
Euphocyp	*Euphorbia cyparissias*	Plantae	Magnoliophyta	Magnoliopsida	Euphorbiales	Euphorbiaceae	Euphorbia L.
Euphoesu	*Euphorbia esula*	Plantae	Magnoliophyta	Magnoliopsida	Euphorbiales	Euphorbiaceae	Euphorbia L.
Festurub	*Festuca rubra*	Plantae	Magnoliophyta	Liliopsida	Cyperales	Poaceae	Festuca
Galeotet	*Galeopsis tetrahit*	Plantae	Magnoliophyta	Magnoliopsida	Lamiales	Lamiaceae	Galeopsis
Galiuapa	*Galium aparine*	Plantae	Magnoliophyta	Magnoliopsida	Rubiales	Rubiaceae	Galium
Galiumol	*Galium mollugo*	Plantae	Magnoliophyta	Magnoliopsida	Rubiales	Rubiaceae	Galium
Geranpus	*Geranium pusillum*	Plantae	Magnoliophyta	Magnoliopsida	Geraniales	Geraniaceae	Geranium

Glechhed	*Glechoma hederacea*	Plantae	Magnoliophyta	Magnoliopsida	Lamiales	Lamiaceae	Glechoma
Hernigla	*Herniaria glabra*	Plantae	Magnoliophyta	Magnoliopsida	Caryophyllales	Caryophyllaceae	Herniaria
Hyperper	*Hypericum perforatum*	Plantae	Magnoliophyta	Magnoliopsida	Theales	Clusiaceae	Hypericum
Iris pse	*Iris pseudacorus*	Plantae	Magnoliophyta	Liliopsida	Liliales	Iridaceae	Iris
Linarvul	*Linaria vulgaris*	Plantae	Magnoliophyta	Magnoliopsida	Scrophulariales	Scrophulariaceae	Linaria
Loliuper	*Lolium perenne*	Plantae	Magnoliophyta	Liliopsida	Cyperales	Poaceae	Lolium
Lycopeur	*Lycopus europaeus*	Plantae	Magnoliophyta	Magnoliopsida	Lamiales	Lamiaceae	Lycopus
Lythrsal	*Lythrum salicaria*	Plantae	Magnoliophyta	Magnoliopsida	Myrtales	Lythraceae	Lythrum
Matrimar	*Matricaria maritima*	Plantae	Magnoliophyta	Magnoliopsida	Asterales	Asteraceae	Matricaria
Mediclup	*Medicago lupulina*	Plantae	Magnoliophyta	Magnoliopsida	Rosales	Fabaceae	Medicago
Melilalt	*Melilotus altissima*	Plantae	Magnoliophyta	Magnoliopsida	Rosales	Fabaceae	Melilotus P. Mill.
Menthaqu	*Mentha aquatica*	Plantae	Magnoliophyta	Magnoliopsida	Lamiales	Lamiaceae	Mentha
Myosoarv	*Myosotis arvensis*	Plantae	Magnoliophyta	Magnoliopsida	Lamiales	Boraginaceae	Myosotis
Myosol-c	*Myosotis laxa (subsp. cespitosa)*	Plantae	Magnoliophyta	Magnoliopsida	Lamiales	Boraginaceae	Myosotis
Odontver	*Odontites vernus*	Plantae	Magnoliophyta	Magnoliopsida	Scrophulariales	Scrophulariaceae	Odontites
Odontv-s	*Odontites vernus subsp. serotinus*	Plantae	Magnoliophyta	Magnoliopsida	Scrophulariales	Scrophulariaceae	Odontites
Oenotbie	*Oenothera biennis*	Plantae	Magnoliophyta	Magnoliopsida	Myrtales	Onagraceae	Oenothera
Pastisat	*Pastinaca sativa*	Plantae	Magnoliophyta	Magnoliopsida	Apiales	Apiaceae	Pastinaca
Phalaaru	*Phalaris arundinacea*	Plantae	Magnoliophyta	Liliopsida	Cyperales	Poaceae	Phalaris
Phleupra	*Phleum pratense*	Plantae	Magnoliophyta	Liliopsida	Cyperales	Poaceae	Phleum
Plantlan	*Plantago lanceolata*	Plantae	Magnoliophyta	Liliopsida	Plantaginales	Plantaginaceae	Plantago
Plantmaj	*Plantago major*	Plantae	Magnoliophyta	Magnoliopsida	Plantaginales	Plantaginaceae	Plantago
Poa ann	*Poa annua*	Plantae	Magnoliophyta	Liliopsida	Cyperales	Poaceae	Poa
Poa pra	*Poa pratensis*	Plantae	Magnoliophyta	Liliopsida	Cyperales	Poaceae	Poa
Poa tri	*Poa trivialis*	Plantae	Magnoliophyta	Liliopsida	Cyperales	Poaceae	Poa
Polynper	*Polygonum persicaria*	Plantae	Magnoliophyta	Magnoliopsida	Polygonales	Polygonaceae	Polygonum
Potenans	*Potentilla anserina*	Plantae	Magnoliophyta	Magnoliopsida	Rosales	Rosaceae	Potentilla
Potenrep	*Potentilla reptans*	Plantae	Magnoliophyta	Magnoliopsida	Rosales	Rosaceae	Potentilla
Prunevul	*Prunella vulgaris*	Plantae	Magnoliophyta	Magnoliopsida	Lamiales	Lamiaceae	Prunella
Ranunrep	*Ranunculus repens*	Plantae	Magnoliophyta	Magnoliopsida	Ranunculales	Ranunculaceae	Ranunculus

Roripaus	*Rorippa austriaca*	Plantae	Magnoliophyta	Magnoliopsida	Capparales	Brassicaceae	Rorippa
Rubuscae	*Rubus caesius*	Plantae	Magnoliophyta	Magnoliopsida	Rosales	Rosaceae	Rubus
Rumexace	*Rumex acetosa*	Plantae	Magnoliophyta	Magnoliopsida	Polygonales	Polygonaceae	Rumex
Rumexcri	*Rumex crispus*	Plantae	Magnoliophyta	Magnoliopsida	Polygonales	Polygonaceae	Rumex
Rumexobt	*Rumex obtusifolius*	Plantae	Magnoliophyta	Magnoliopsida	Polygonales	Polygonaceae	Rumex
Saponoff	*Saponaria officinalis*	Plantae	Magnoliophyta	Magnoliopsida	Caryophyllales	Caryophyllaceae	Saponaria
Seneceru	*Senecio erucifolius*	Plantae	Magnoliophyta	Magnoliopsida	Asterales	Asteraceae	Senecio
Senecina	*Senecio inaequidens*	Plantae	Magnoliophyta	Magnoliopsida	Asterales	Asteraceae	Senecio
Senecjac	*Senecio jacobaea*	Plantae	Magnoliophyta	Magnoliopsida	Asterales	Asteraceae	Senecio
Solandul	*Solanum dulcamara*	Plantae	Magnoliophyta	Magnoliopsida	Solanales	Solanaceae	Solanum
Solidcan	*Solidago canadensis*	Plantae	Magnoliophyta	Magnoliopsida	Asterales	Asteraceae	Solidago
Stellaqu	*Stellaria aquatica*	Plantae	Magnoliophyta	Magnoliopsida	Caryophyllales	Caryophyllaceae	Stellaria
Tanacvul	*Tanacetum vulgare*	Plantae	Magnoliophyta	Magnoliopsida	Asterales	Asteraceae	Tanacetum
Taraxoff	*Taraxacum officinale s.s.*	Plantae	Magnoliophyta	Magnoliopsida	Asterales	Asteraceae	Taraxacum
Trifofra	*Trifolium fragiferum*	Plantae	Magnoliophyta	Magnoliopsida	Rosales	Fabaceae	Trifolium
Triforep	*Trifolium repens*	Plantae	Magnoliophyta	Magnoliopsida	Rosales	Fabaceae	Trifolium
Urticdio	*Urtica dioica*	Plantae	Magnoliophyta	Magnoliopsida	Urticales	Urticaceae	Urtica
Verbanig	*Verbascum nigrum*	Plantae	Magnoliophyta	Magnoliopsida	Scrophulariales	Scrophulariaceae	Verbascum

Table V: Taxonomical classification for the vegetation species in the Millingerwaard

APPENDIX III
VEGETATION COMMUNITIES – RELEVEES:

CLUSTER NUMBER	Specie	*Cotyledons*	*Type veg.*	Fld. Spec
1	*Medicagini-Avenetum pubescentis*	Dicot.	Forb / herb	
	Bromo inermis	Monocot.	Graminoid	
	Eryngietum campestris	Dicot.	Forb / herb	
2	*Lolio*	Monocot.	Graminoid	
	Potentillion anserinae	Dicot.	Forb / herb	
	Bromo inermis	Monocot.	Graminoid	
	Eryngietum campestris	Dicot.	Forb / herb	
3	*Cynodon dactylon*	Monocot.	Graminoid	
	Euphorbia esula	Dicot.	Forb / herb	
	Bromo inermis	Monocot.	Graminoid	
	Eryngietum campestris	Dicot.	Forb / herb	
4	*Medicagini-Avenetum pubescentis*	Dicot.	Forb / herb	relevee15
	Bromo inermis	Monocot.	Graminoid	
	Eryngietum campestris	Dicot.	Forb / herb	
	Cynodon dactylon	Monocot.	Graminoid	
5	*Bromo inermis*	Monocot.	Graminoid	relevee18
	Eryngietum campestris	Dicot.	Forb / herb	
6	*Medicagini-Avenetum pubescentis*	Dicot.	Forb / herb	relevee17
	Bromo inermis	Monocot.	Graminoid	
	Eryngietum campestris	Dicot.	Forb / herb	
	Oenothera erytrosepala	Dicot.	Forb / herb	
	Sedum acre	Dicot.	Forb / herb	
7	*Bromo inermis*	Monocot.	Graminoid	relevee20
	Eryngietum campestris	Dicot.	Forb / herb	
	Medicagini-Avenetum pubescentis	Dicot.	Forb / herb	
8	*Medicagini-Avenetum pubescentis*	Dicot.	Forb / herb	relevee14, 19
	Bromo inermis	Monocot.	Graminoid	
	Eryngietum campestris	Dicot.	Forb / herb	
	Euphorbia cyparissias	Dicot.	Forb / herb	
	Medicago falcata	Dicot.	Forb / herb	
9	*Arrhenatheretum elatioris*	Monocot.	Graminoid	relevee13, 21
10	*Ranunculo*	Dicot.	Forb / herb	relevee2
	Alopecuretum geniculati	Monocot.	Graminoid	
	Trifolium repens	Dicot.	Forb / herb	
11	*Ranunculo*	Dicot.	Forb / herb	relevee5
	Alopecuretum geniculati	Monocot.	Graminoid	
12	*Chenopodietum rubri*	Dicot.	Forb / herb	
13	*Cirsium arvense*	Dicot.	Forb / herb	
	Polygonum amphibium	Dicot.	Forb / herb	
	Artemisietia vulgaris	Dicot.	Forb / herb	
14	*Urtica dioica*	Dicot.	Forb / herb	relevee3 , 22
15	*Rubus caesius*	Dicot.	Shrub	relevee4, 6, 9, 11
16	*Calamagrostis epigejos*	Monocot	Graminoid	relevee10
	Epilobium hirsutum	Dicot.	Forb / herb	
17	*Sambucus nigra*	Dicot.	Forb / herb	relevee12
18	*Ranunculo*	Dicot.	Forb / herb	
	Alopecuretum geniculati	Monocot.	Graminoid	
	Rubus caesius	Dicot	Shrub	
19	*Brassica nigra*	Dicot.	Forb / herb	
	Ranunculo	Dicot.	Forb / herb	
	Alopecuretum geniculati	Monocot.	Graminoid	
20	*Ranunculo*	Dicot.	Forb / herb	
	Alopecuretum geniculati	Monocot.	Graminoid	
	Lythrum salicaria	Dicot.	Forb / herb	
	Mentha aquatica	Dicot.	Forb / herb	
21	*Ranunculo*	Dicot.	Forb / herb	
	Alopecuretum geniculati	Monocot.	Graminoid	
22	*Mentha aquatica*	Dicot.	Forb / herb	relevee8
	Lycopus europaeus	Dicot.	Forb / herb	
23	*Rorippo*	Dicot.	Forb / herb	relevee7
	Oenanthetum aquaticae	Dicot.	Forb / herb	
24	*Ulmus minor*	Dicot.	Forb / herb	

Table VI: Correspondence between measured relevees and vegetation communities

APPENDIX IV:
SPATIAL COBERTURE PER SPECIE AND RELEVEE

Relevee	**2**	**3**	**4**	**5**	**6**	**7**	**8**	**9**	**10**	**11**	**12**	**13**	**14**	**15**	**16**	**17**	**18**	**19**	**20**	**21**	**22**	
Achilmil	0	0	0	0	0	0	0	0	0	0	0	3	0	2	0	0	0	3	2	18	0	*Achillea millefolium*
Agrossto	2	0	0	3	0	0	0	0	0	0	0	3	0	0	0	0	0	0	0	18	2	*Agrostis stolonifera*
Arctilap	2	3	0	2	0	3	8	8	2	0	0	2	0	0	0	0	0	0	0	1	0	*Arctium lappa*
Arrheela	0	0	0	0	0	0	0	0	0	0	3	0	0	0	0	0	0	0	0	1	0	*Arrhenatherum elatius*
Atrippat	0	0	0	0	0	0	0	0	0	0	0	0	0	0	0	1	1	0	0	0	0	*Atriplex patula*
Brassnig	0	3	18	0	0	0	3	2	2	0	0	0	0	0	0	0	0	2	0	0	8	*Brassica nigra*
Bromuine	0	0	0	0	0	0	0	0	0	0	0	0	8	2	0	0	0	0	3	0	0	*Bromus inermis*
Calamepi	0	2	0	0	0	0	0	0	88	3	18	0	8	3	0	38	3	4	68	0	0	*Calamagrostis epigejos*
Calyssep	0	3	0	0	0	0	0	3	0	0	0	0	0	0	0	0	0	0	0	0	0	*Calystegia sepium*
Cardunut	0	0	0	0	0	0	0	0	0	0	0	0	0	2	0	0	0	0	2	0	0	*Carduus nutans*
Carexhir	0	0	0	0	2	0	0	0	3	0	2	0	0	8	0	3	3	0	0	0	0	*Carex hirta*
Cerasfon	0	0	0	0	0	0	0	0	0	0	0	0	2	2	0	0	0	0	2	0	0	*Cerastium fontanum*
Cirsiarv	2	8	8	8	2	38	18	3	8	2	0	0	0	1	18	0	0	8	0	2	8	*Cirsium arvense*
Cirsivul	0	0	3	0	0	0	0	0	0	0	0	0	0	0	0	0	0	0	0	2	0	*Cirsium vulgare*
Cratamon	0	0	0	0	2	0	0	0	0	0	0	0	0	0	0	0	0	0	0	0	0	*Crataegus monogyna*
Cynoddac	0	0	0	0	0	0	0	0	0	0	0	18	0	68	0	0	0	0	0	0	0	*Cynodon dactylon*
Dactyglo	0	0	0	0	0	0	0	2	0	0	0	38	0	0	1	0	0	0	2	3	0	*Dactylis glomerata*
Dipsaful	0	0	0	0	0	0	0	0	0	0	0	0	0	0	0	0	0	0	0	2	0	*Dipsacus fullonum*
Elymurep	18	4	0	2	2	0	4	0	0	0	0	2	0	0	0	0	2	0	2	3	0	*Elymus repens*
Epilohir	0	0	0	0	0	2	2	0	8	0	0	0	0	0	0	0	0	0	0	0	0	*Epilobium hirsutum*
Epilotet	0	0	0	0	0	18	38	0	2	0	0	0	0	0	0	0	0	0	0	0	0	*Epilobium tetragonum*
Equisarv	0	0	0	0	0	0	0	0	0	0	0	0	0	0	3	0	0	0	0	0	0	*Equisetum arvense*
Erigecan	0	0	0	0	0	0	0	0	0	0	0	0	2	2	0	0	0	1	2	0	2	*Erigeron canadensis*
Eryngcam	0	0	0	0	0	0	0	0	0	0	0	0	18	38	0	38	18	38	0	3	0	*Eryngium campestre*
Euphocyp	0	0	0	0	0	0	0	0	0	0	0	0	2	0	0	0	0	0	0	0	0	*Euphorbia cyparissias*
Euphoesu	0	2	0	0	0	0	0	0	2	0	0	0	38	0	0	0	0	0	1	0	0	*Euphorbia esula*
Festurub	0	0	0	0	0	0	0	0	0	0	0	0	8	4	2	4	3	68	0	8	0	*Festuca rubra*
Galeotet	0	0	0	0	0	0	0	0	2	2	0	0	0	0	0	0	0	0	0	0	0	*Galeopsis tetrahit*
Galiuapa	0	0	2	0	0	0	0	0	3	2	2	0	0	0	0	0	0	0	0	0	0	*Galium aparine*
Galiumol	0	0	0	0	0	0	2	0	0	0	0	0	0	0	0	0	0	0	8	0	0	*Galium mollugo*

Relevee	**2**	**3**	**4**	**5**	**6**	**7**	**8**	**9**	**10**	**11**	**12**	**13**	**14**	**15**	**16**	**17**	**18**	**19**	**20**	**21**	**22**	
Geranpus	0	0	0	2	0	0	0	0	0	0	0	0	0	0	0	0	0	0	0	0	0	*Geranium pusillum*
Glechhed	2	2	2	0	38	0	8	38	38	38	8	0	0	0	0	0	0	0	0	0	2	*Glechoma hederacea*
Hernigla	0	0	0	0	0	0	0	0	0	0	0	8	2	0	0	2	0	18	0	0	2	*Herniaria glabra*
Hyperper	0	0	0	0	0	0	0	0	0	0	0	0	0	1	0	0	0	0	0	2	0	*Hypericum perforatum*
Iris pse	0	0	0	0	0	0	0	1	0	0	0	0	0	0	0	0	0	0	0	0	0	*Iris pseudacorus*
Linarvul	0	0	0	0	0	0	0	0	0	0	0	0	1	0	0	0	0	0	0	0	0	*Linaria vulgaris*
Loliuper	38	0	0	0	0	0	0	0	0	0	0	0	0	0	0	0	0	0	0	2	0	*Lolium perenne*
Lycopeur	0	0	0	0	0	2	2	0	0	0	0	0	0	0	0	0	0	0	0	0	0	*Lycopus europaeus*
Lythrsal	0	2	0	0	0	38	0	0	0	0	0	0	0	0	0	0	0	0	0	0	0	*Lythrum salicaria*
Matrimar	0	0	0	0	0	2	2	0	0	0	0	0	0	0	0	0	0	0	2	0	0	*Matricaria maritima*
Mediclup	0	0	0	0	0	0	0	0	0	0	0	0	0	0	0	0	0	0	0	8	0	*Medicago lupulina*
Melilalt	0	0	0	0	0	0	0	0	0	0	0	0	2	0	0	0	0	2	0	0	0	*Melilotus altissima*
Menthaqu	0	0	0	0	0	68	38	0	0	0	0	0	0	0	0	0	0	0	0	0	0	*Mentha aquatica*
Myosoarv	0	0	0	0	0	0	0	0	0	0	0	0	0	0	0	0	0	0	1	0	0	*Myosotis arvensis*
Myosol-c	0	0	0	0	0	2	0	0	0	0	0	0	0	0	0	0	0	0	0	0	0	*Myosotis laxa (subsp. cespitosa)*
Odontver	2	2	0	0	0	0	2	0	0	0	0	0	0	0	0	0	0	0	0	0	0	*Odontites vernus*
Odontv-s	0	0	0	2	0	0	0	0	0	0	0	0	0	0	0	0	0	0	0	0	0	*Odontites vernus (subsp.serotinus)*
Oenotbie	0	0	0	0	0	0	0	0	0	0	0	0	0	0	0	0	0	2	0	0	3	*Oenothera biennis*
Pastisat	0	0	0	0	0	0	0	0	0	0	0	0	0	0	0	0	0	0	0	2	0	*Pastinaca sativa*
Phalaaru	0	0	0	0	0	2	0	0	0	0	0	0	0	0	0	0	0	0	0	0	0	*Phalaris arundinacea*
Phleupra	0	3	0	18	0	0	0	0	0	0	0	0	0	0	0	0	0	0	0	0	0	*Phleum pratense*
Plantlan	2	0	0	0	0	0	0	0	0	0	0	0	0	0	0	2	0	0	0	0	0	*Plantago lanceolata*
Plantmaj	2	0	0	0	0	0	0	0	0	0	0	0	0	0	0	0	0	0	0	0	0	*Plantago major*
Poa ann	18	0	0	38	0	0	0	0	0	0	0	0	0	0	0	0	0	0	0	0	0	*Poa annua*
Poa pra	0	0	0	2	0	0	0	0	0	0	4	0	0	0	0	0	0	0	4	0	0	*Poa pratensis*
Poa tri	2	4	0	0	2	3	0	4	2	4	0	0	2	2	0	0	0	0	0	18	2	*Poa trivialis*
Polynper	0	2	0	0	0	0	0	0	0	0	0	0	0	0	3	0	0	0	0	0	3	*Polygonum persicaria*
Potenans	2	3	0	3	0	0	0	0	0	0	0	0	0	0	0	0	0	0	2	0	3	*Potentilla anserina*
Potenrep	0	18	0	0	18	0	18	0	18	3	3	68	38	1	0	0	0	0	0	1	2	*Potentilla reptans*
Prunevul	0	0	0	0	0	0	0	0	0	0	0	0	0	2	0	0	0	0	0	0	0	*Prunella vulgaris*

Relevee	**2**	**3**	**4**	**5**	**6**	**7**	**8**	**9**	**10**	**11**	**12**	**13**	**14**	**15**	**16**	**17**	**18**	**19**	**20**	**21**	**22**	
Ranunrep	0	0	0	2	0	0	2	0	0	0	0	0	0	0	0	0	0	0	0	2	0	*Ranunculus repens*
Roripaus	0	0	0	0	0	0	0	0	0	0	2	0	0	0	0	0	0	0	0	0	0	*Rorippa austriaca*
Rubuscae	0	38	88	0	88	0	0	88	8	88	88	0	0	0	0	3	0	0	0	0	0	*Rubus caesius*
Rumexace	0	0	0	0	0	0	0	0	0	0	0	0	0	3	0	18	0	0	38	0	0	*Rumex acetosa*
Rumexcri	0	2	0	0	0	3	0	0	0	0	0	0	0	0	0	0	0	0	0	0	0	*Rumex crispus*
Rumexobt	0	0	0	0	0	0	0	0	0	0	0	0	0	0	0	0	0	0	0	0	8	*Rumex obtusifolius*
Saponoff	0	0	0	0	0	0	0	0	0	0	0	0	0	0	0	0	18	0	0	0	8	*Saponaria officinalis*
Seneceru	0	0	0	0	0	3	0	0	0	0	0	0	0	0	0	0	0	0	0	0	0	*Senecio erucifolius*
Senecina	0	0	0	0	0	0	0	0	0	0	0	0	0	2	0	3	2	0	18	0	38	*Senecio inaequidens*
Senecjac	0	0	0	0	0	0	0	0	0	0	0	0	0	2	0	3	0	1	0	2	0	*Senecio jacobaea*
Solandul	0	0	2	0	0	0	0	0	0	0	0	0	0	0	0	0	0	0	0	0	0	*Solanum dulcamara*
Solidcan	0	0	2	0	0	2	2	0	0	0	0	0	0	0	0	0	0	0	0	0	0	*Solidago canadensis*
Stellaqu	0	0	0	0	0	8	8	0	0	0	0	0	0	0	0	0	0	0	0	0	0	*Stellaria aquatica*
Tanacvul	0	0	0	0	0	0	0	0	0	0	0	0	0	2	0	0	0	0	0	2	0	*Tanacetum vulgare*
Taraxoff	18	0	0	2	0	0	0	0	0	0	0	3	0	0	0	0	0	0	0	3	0	*Taraxacum officinale s.s.*
Trifofra	3	0	0	0	0	0	0	0	0	0	0	0	0	0	0	0	0	0	0	0	0	*Trifolium fragiferum*
Triforep	68	0	0	68	0	0	0	0	0	0	0	3	0	3	0	0	0	0	0	38	0	*Trifolium repens*
Urticdio	0	18	18	0	3	0	0	3	8	2	2	2	2	0	0	0	0	0	0	0	38	*Urtica dioica*
Verbanig	0	0	0	0	0	0	0	0	0	0	0	0	0	2	0	0	0	0	0	0	2	*Verbascum nigrum*

Table VII: Spatial abundance of species per relevee (The values express percentage of spatial coverage per species and relevee)

APPENDIX V:

MEASURED AND SIMULATED REFLECTANCE SPECTRA (*CANOPY LEVEL*)

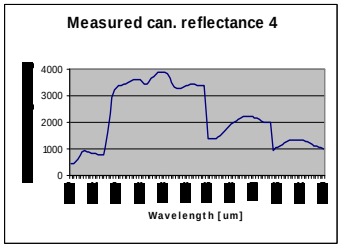

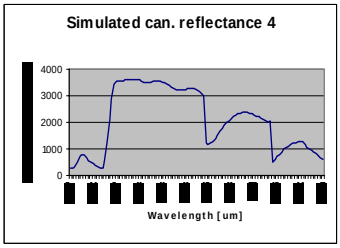

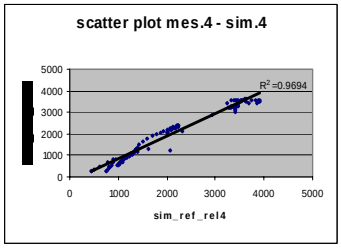

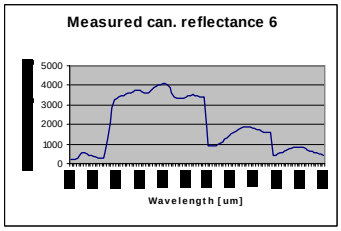

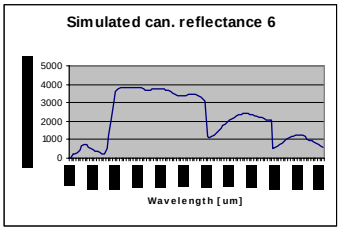

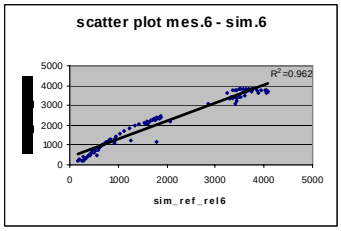

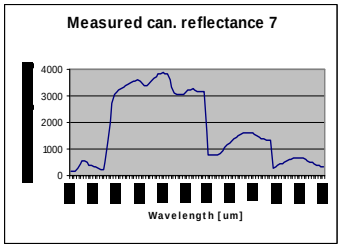

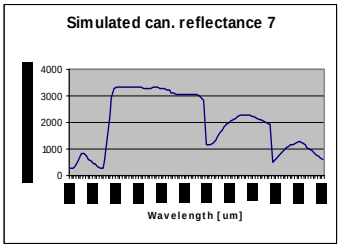

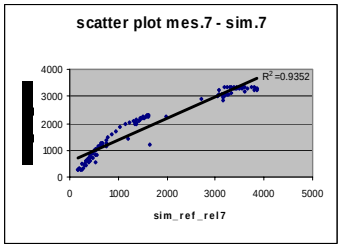

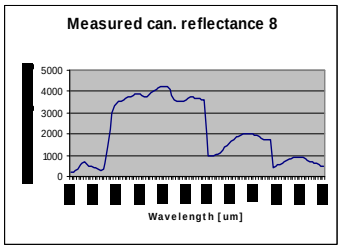

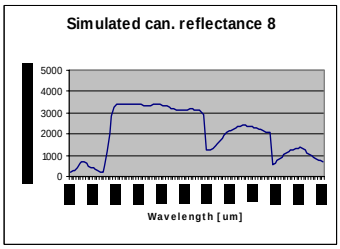

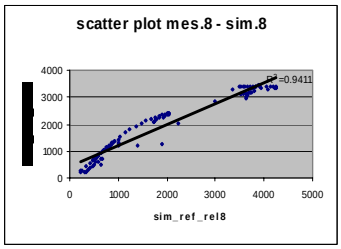

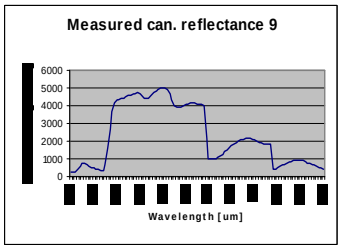

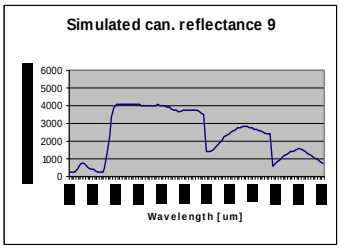

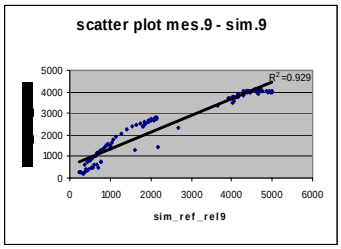

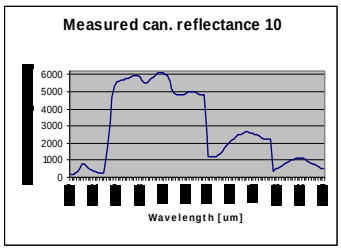

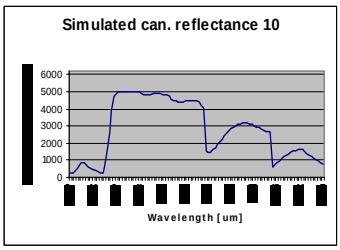

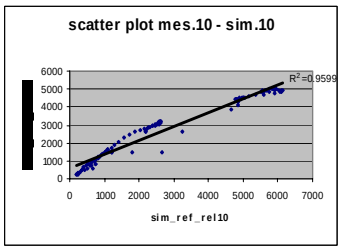

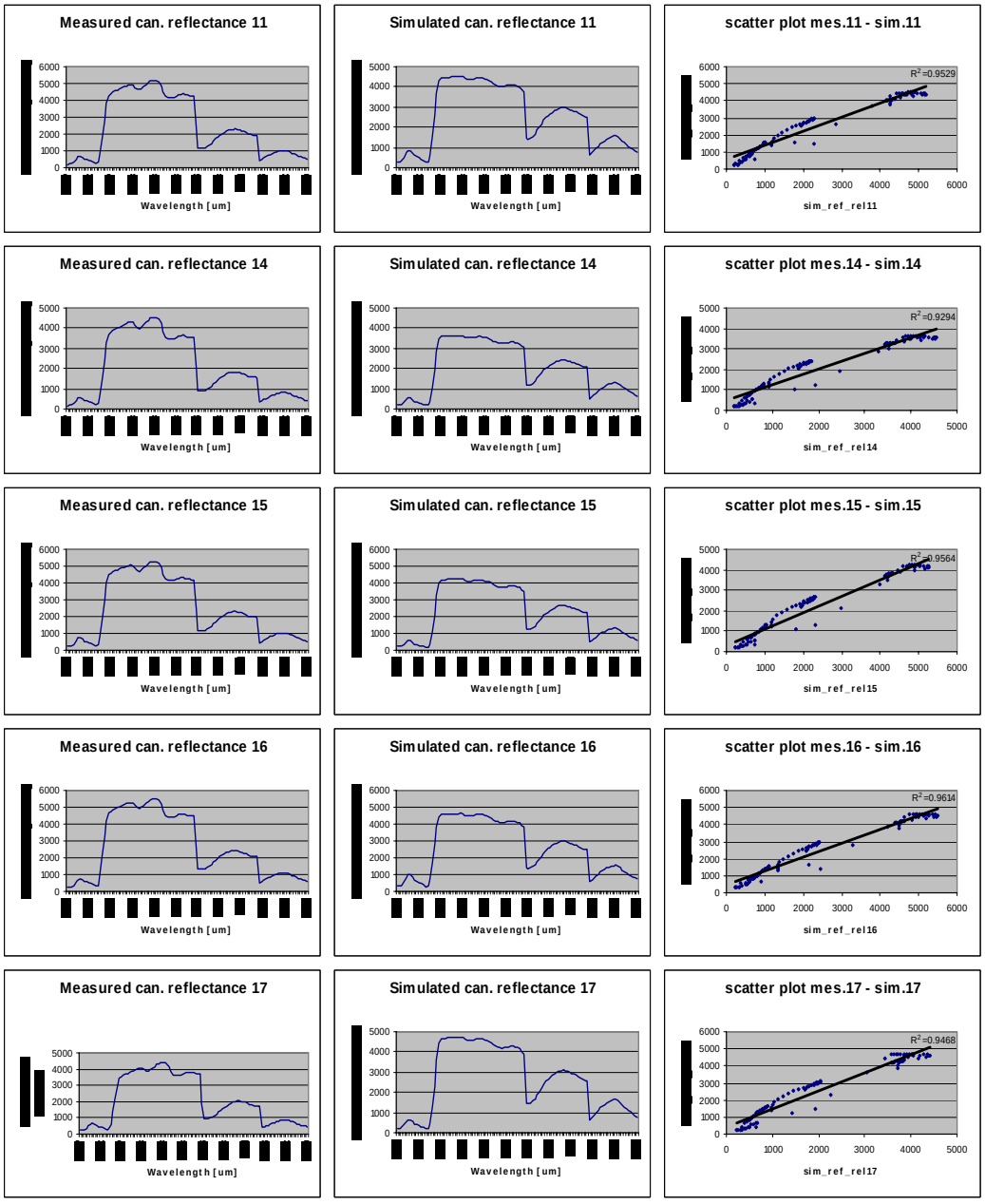

Figure III: Correlation between simulated and measured spectra for vegetation communities

APPENDIX VI:
MEASURED AND SIMULATED REFLECTANCE SPECTRA (*SPECIES LEVEL*)

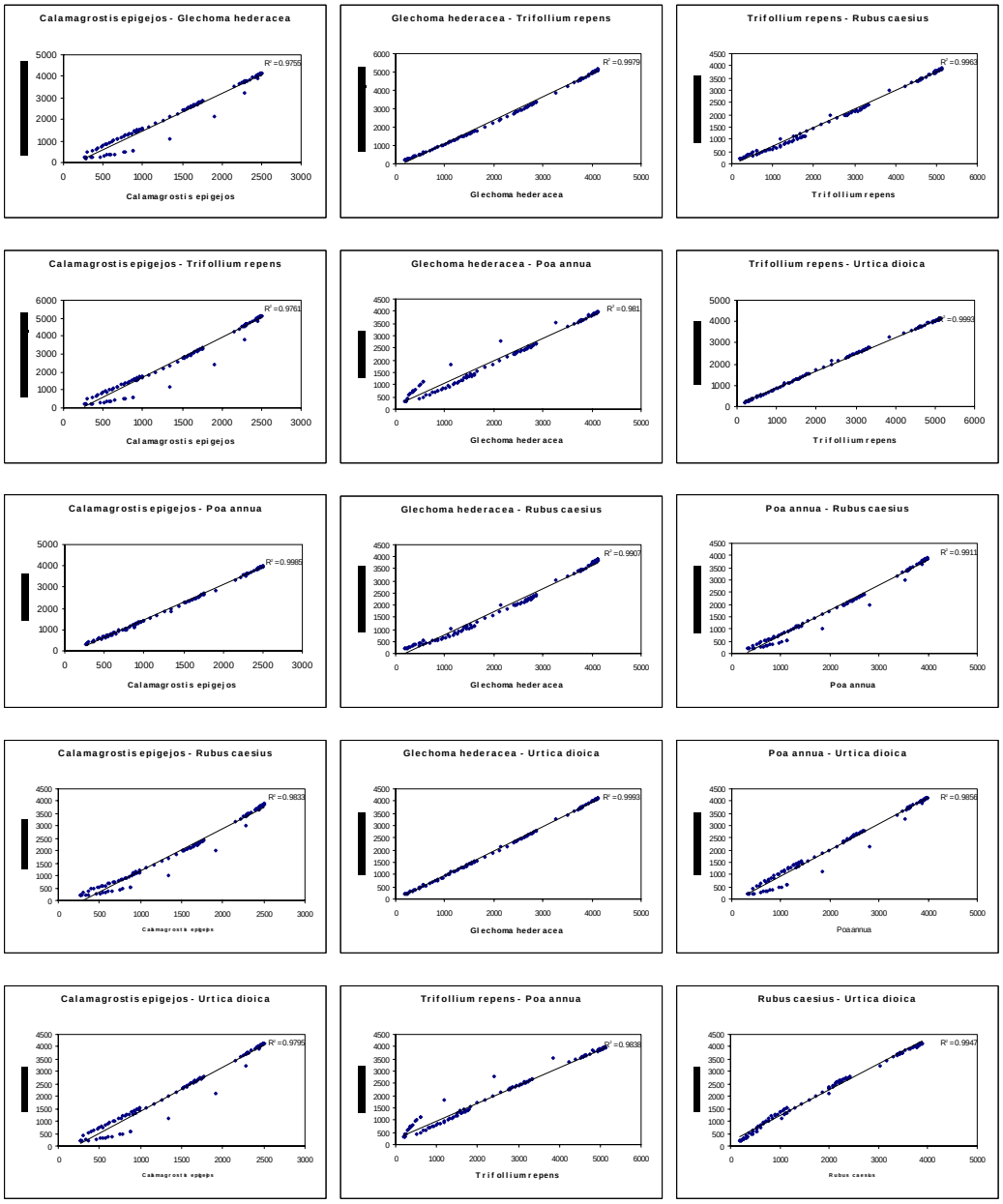

Figure IV: Correlation between simulated and measured spectra for vegetation species

APPENDIX VII:

UNCONSTRAINED LINEAR SPECTRAL UNMIXING AT THE VEGETATION COMMUNITY LEVEL

Area - Vegetation community 4

Spatial abundance map for Community 4 (sim), derived from Hymap data Millingerwaard, The Netherlands

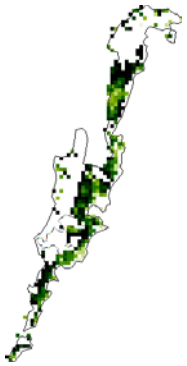

Spatial abundance map for Community 4 (im), derived from Hymap data Millingerwaard, The Netherlands

Spatial abundance map for Community 4 (can), derived from Hymap data Millingerwaard, The Netherlands

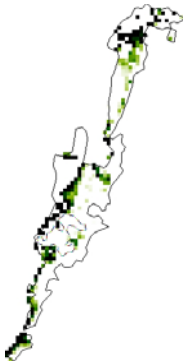

Spatial abundance map for Community 4 (can), derived from Hymap data Millingerwaard, The Netherlands

Spatial abundance map for Community 6 (sim), derived from Hymap data Millingerwaard, The Netherlands

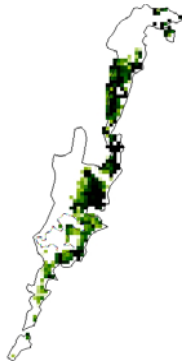

Spatial abundance map for Community 6 (im), derived from Hymap data Millingerwaard, The Netherlands

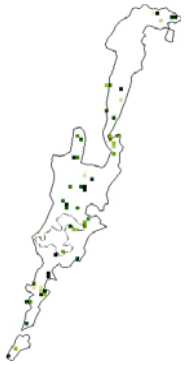

Spatial abundance map for Community 10 (sim), derived from Hymap data Millingerwaard, The Netherlands

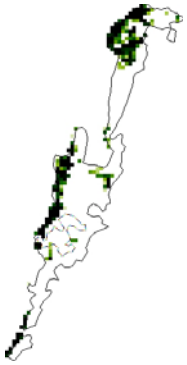

Spatial abundance map for Community 10 (can), derived from Hymap data Millingerwaard, The Netherlands

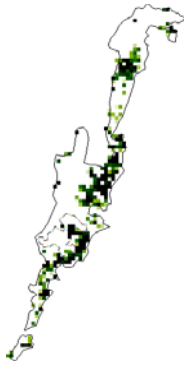

Spatial abundance map for Community 10 (im), derived from Hymap data Millingerwaard, The Netherlands

Spatial abundance map for Community 11 (sim), derived from Hymap data Millingerwaard, The Netherlands

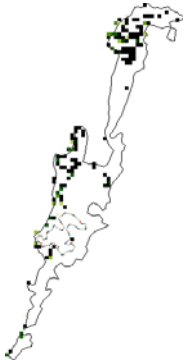

Spatial abundance map for Community 11 (can), derived from Hymap data Millingerwaard, The Netherlands

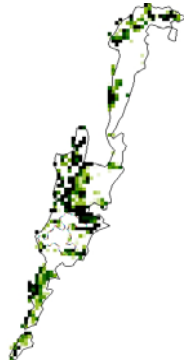

Spatial abundance map for Community 11 (im), derived from Hymap data Millingerwaard, The Netherlands

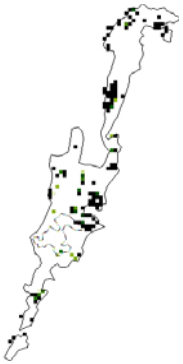

Spatial abundance map for Community 15 (sim), derived from Hymap data Millingerwaard, The Netherlands

Spatial abundance map for Community 15 (can), derived from Hymap data Millingerwaard, The Netherlands

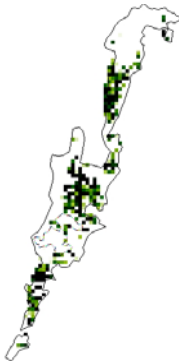

Spatial abundance map for Community 15 (im), derived from Hymap data Millingerwaard, The Netherlands

Spatial abundance map for Community 16 (sim), derived from Hymap data Millingerwaard, The Netherlands

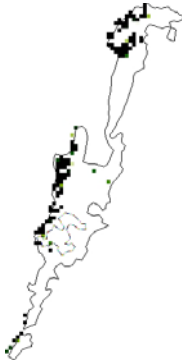

Spatial abundance map for Community 16 (can), derived from Hymap data Millingerwaard, The Netherlands

Spatial abundance map for Community 16 (im), derived from Hymap data Millingerwaard, The Netherlands

Area - Vegetation community 6

Spatial abundance map for Community 4 (sim), derived from Hymap data Millingerwaard, The Netherlands

Spatial abundance map for Community 4 (can), derived from Hymap data Millingerwaard, The Netherlands

Spatial abundance map for Community 4 (im), derived from Hymap data Millingerwaard, The Netherlands

Spatial abundance map for Community 6 (sim), derived from Hymap data Millingerwaard, The Netherlands

Spatial abundance map for Community 6 (can), derived from Hymap data Millingerwaard, The Netherlands

Spatial abundance map for Community 6 (im), derived from Hymap data Millingerwaard, The Netherlands

Spatial abundance map for Community 10 (sim), derived from Hymap data Millingerwaard, The Netherlands

Spatial abundance map for Community 10 (can), derived from Hymap data Millingerwaard, The Netherlands

Spatial abundance map for Community 10 (im), derived from Hymap data Millingerwaard, The Netherlands

Spatial abundance map for Community 11 (sim), derived from Hymap data Millingerwaard, The Netherlands

Spatial abundance map for Community 11 (can), derived from Hymap data Millingerwaard, The Netherlands

Spatial abundance map for Community 11 (im), derived from Hymap data Millingerwaard, The Netherlands

Spatial abundance map for Community 15 (sim), derived from Hymap data Millingerwaard, The Netherlands

Spatial abundance map for Community 15 (can), derived from Hymap data Millingerwaard, The Netherlands

Spatial abundance map for Community 15 (im), derived from Hymap data Millingerwaard, The Netherlands

Spatial abundance map for Community 16 (sim), derived from Hymap data Millingerwaard, The Netherlands

Spatial abundance map for Community 16 (can), derived from Hymap data Millingerwaard, The Netherlands

Spatial abundance map for Community 16 (im), derived from Hymap data Millingerwaard, The Netherlands

Area - Vegetation community 10

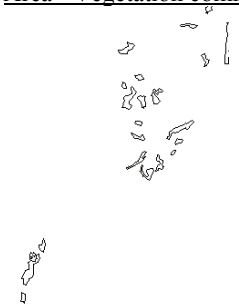

Spatial abundance map for Community 4 (sim), derived from Hymap data Millingerwaard, The Netherlands

Spatial abundance map for Community 4 (can), derived from Hymap data Millingerwaard, The Netherlands

Spatial abundance map for Community 4 (im), derived from Hymap data Millingerwaard, The Netherlands

Spatial abundance map for Community 6 (sim), derived from Hymap data Millingerwaard, The Netherlands

Spatial abundance map for Community 6 (can), derived from Hymap data Millingerwaard, The Netherlands

Spatial abundance map for Community 6 (im), derived from Hymap data Millingerwaard, The Netherlands

Spatial abundance map for Community 10 (sim), derived from Hymap data Millingerwaard, The Netherlands

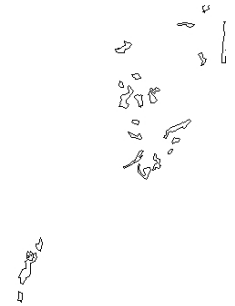

Spatial abundance map for Community 10 (can), derived from Hymap data Millingerwaard, The Netherlands

Spatial abundance map for Community 10 (im), derived from Hymap data Millingerwaard, The Netherlands

Spatial abundance map for Community 11 (sim), derived from Hymap data Millingerwaard, The Netherlands

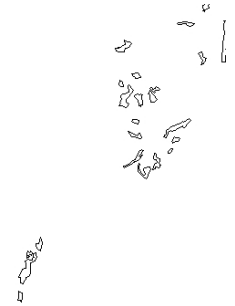

Spatial abundance map for Community 11 (can), derived from Hymap data Millingerwaard, The Netherlands

Spatial abundance map for Community 11 (im), derived from Hymap data Millingerwaard, The Netherlands

Spatial abundance map for Community 15 (sim), derived from Hymap data Millingerwaard, The Netherlands

Spatial abundance map for Community 15 (can), derived from Hymap data Millingerwaard, The Netherlands

Spatial abundance map for Community 15 (im), derived from Hymap data Millingerwaard, The Netherlands

Spatial abundance map for Community 16 (sim), derived from Hymap data Millingerwaard, The Netherlands

Spatial abundance map for Community 16 (can), derived from Hymap data Millingerwaard, The Netherlands

Spatial abundance map for Community 16 (im), derived from Hymap data Millingerwaard, The Netherlands

Area - Vegetation community 11

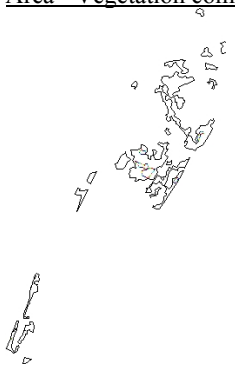

Spatial abundance map for Community 4 (sim), derived from Hymap data Millingerwaard, The Netherlands

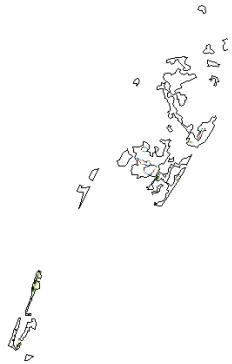

Spatial abundance map for Community 6 (can), derived from Hymap data Millingerwaard, The Netherlands

Spatial abundance map for Community 4 (im), derived from Hymap data Millingerwaard, The Netherlands

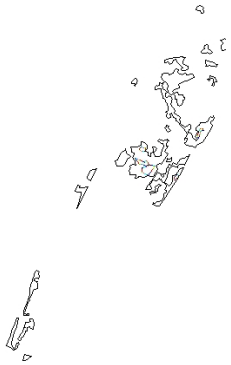

Spatial abundance map for Community 6 (sim), derived from Hymap data Millingerwaard, The Netherlands

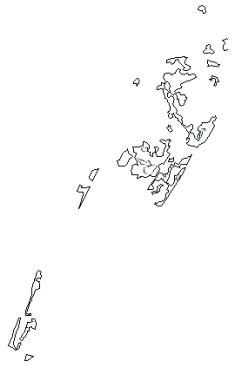

Spatial abundance map for Community 6 (can), derived from Hymap data Millingerwaard, The Netherlands

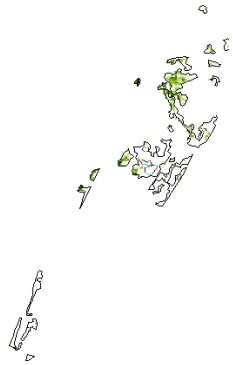

Spatial abundance map for Community 6 (im), derived from Hymap data Millingerwaard, The Netherlands

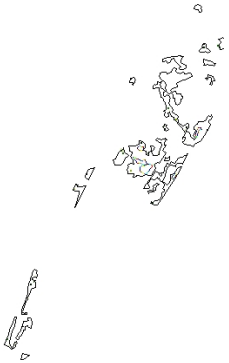

Spatial abundance map for Community 10 (sim), derived from Hymap data Millingerwaard, The Netherlands

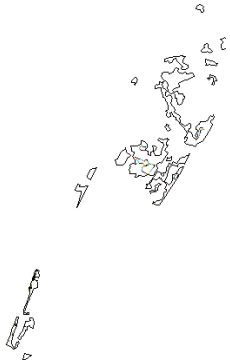

Spatial abundance map for Community 10 (can), derived from Hymap data Millingerwaard, The Netherlands

Spatial abundance map for Community 10 (im), derived from Hymap data Millingerwaard, The Netherlands

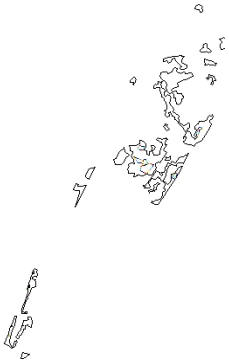

Spatial abundance map for Community 11 (sim), derived from Hymap data Millingerwaard, The Netherlands

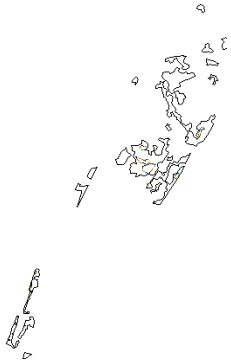

Spatial abundance map for Community 11 (can), derived from Hymap data Millingerwaard, The Netherlands

Spatial abundance map for Community 11 (im), derived from Hymap data Millingerwaard, The Netherlands

Spatial abundance map for Community 15 (sim), derived from Hymap data Millingerwaard, The Netherlands

Spatial abundance map for Community 15 (can), derived from Hymap data Millingerwaard, The Netherlands

Spatial abundance map for Community 15 (im), derived from Hymap data Millingerwaard, The Netherlands

Spatial abundance map for Community 16 (sim), derived from Hymap data Millingerwaard, The Netherlands

Spatial abundance map for Community 16 (can), derived from Hymap data Millingerwaard, The Netherlands

Spatial abundance map for Community 16 (im), derived from Hymap data Millingerwaard, The Netherlands

Area - Vegetation community 15

Spatial abundance map for Community 4 (sim), derived from Hymap data Millingerwaard, The Netherlands

Spatial abundance map for Community 4 (can), derived from Hymap data Millingerwaard, The Netherlands

Spatial abundance map for Community 4 (im), derived from Hymap data Millingerwaard, The Netherlands

Spatial abundance map for Community 6 (sim), derived from Hymap data Millingerwaard, The Netherlands

Spatial abundance map for Community 6 (can), derived from Hymap data Millingerwaard, The Netherlands

Spatial abundance map for Community 6 (im), derived from Hymap data Millingerwaard, The Netherlands

Spatial abundance map for Community 10 (sim), derived from Hymap data Millingerwaard, The Netherlands

Spatial abundance map for Community 10 (can), derived from Hymap data Millingerwaard, The Netherlands

Spatial abundance map for Community 10 (im), derived from Hymap data Millingerwaard, The Netherlands

Spatial abundance map for Community 11 (sim), derived from Hymap data Millingerwaard, The Netherlands

Spatial abundance map for Community 11 (can), derived from Hymap data Millingerwaard, The Netherlands

Spatial abundance map for Community 11 (im), derived from Hymap data Millingerwaard, The Netherlands

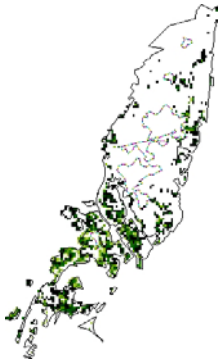

Spatial abundance map for Community 15 (sim), derived from Hymap data Millingerwaard, The Netherlands

Spatial abundance map for Community 15 (can), derived from Hymap data Millingerwaard, The Netherlands

Spatial abundance map for Community 15 (im), derived from Hymap data Millingerwaard, The Netherlands

Spatial abundance map for Community 16 (sim), derived from Hymap data Millingerwaard, The Netherlands

Spatial abundance map for Community 16 (can), derived from Hymap data Millingerwaard, The Netherlands

Spatial abundance map for Community 16 (im), derived from Hymap data Millingerwaard, The Netherlands

Area - Vegetation community 16

Spatial abundance map for Community 4 (sim), derived from Hymap data Millingerwaard, The Netherlands

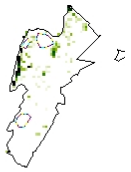

Spatial abundance map for Community 4 (can), derived from Hymap data Millingerwaard, The Netherlands

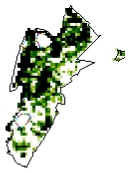

Spatial abundance map for Community 4 (im), derived from Hymap data Millingerwaard, The Netherlands

Spatial abundance map for Community 6 (sim), derived from Hymap data Millingerwaard, The Netherlands

Spatial abundance map for Community 6 (can), derived from Hymap data Millingerwaard, The Netherlands

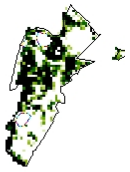

Spatial abundance map for Community 6 (im), derived from Hymap data Millingerwaard, The Netherlands

Spatial abundance map for Community 10 (sim), derived from Hymap data Millingerwaard, The Netherlands

Spatial abundance map for Community 10 (can), derived from Hymap data Millingerwaard, The Netherlands

Spatial abundance map for Community 10 (im), derived from Hymap data Millingerwaard, The Netherlands

Spatial abundance map for Community 11 (sim), derived from Hymap data Millingerwaard, The Netherlands

Spatial abundance map for Community 11 (can), derived from Hymap data Millingerwaard, The Netherlands

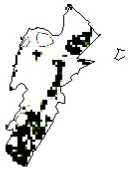

Spatial abundance map for Community 11 (im), derived from Hymap data Millingerwaard, The Netherlands

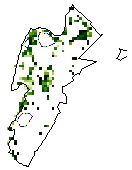

Spatial abundance map for Community 15 (sim), derived from Hymap data Millingerwaard, The Netherlands

Spatial abundance map for Community 15 (can), derived from Hymap data Millingerwaard, The Netherlands

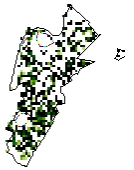

Spatial abundance map for Community 15 (im), derived from Hymap data Millingerwaard, The Netherlands

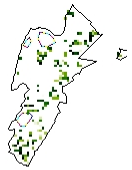

Spatial abundance map for Community 16 (sim), derived from Hymap data Millingerwaard, The Netherlands

Spatial abundance map for Community 16 (can), derived from Hymap data Millingerwaard, The Netherlands

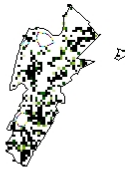

Spatial abundance map for Community 16 (im), derived from Hymap data Millingerwaard, The Netherlands